The Abdus Salam International Centre for Theoretical Physics

2359-21

Joint ICTP-IAEA Workshop on Physics of Radiation Effect and its Simulation for Non-Metallic Condensed Matter

13 - 24 August 2012

Effects of swift heavy ion irradiation and simulation of fission fragment impact

V.A. Skuratov

Joint Institute for Nuclear Research
Dubna
Russia

Strada Costiera, 11 - 34151 - Trieste - Italy • Tel. +39 0402240111 • Fax. +39 040224163 • sci_info@ictp.it • www.ictp.it

ICTP is governed by UNESCO, IAEA, and Italy, and it is a UNESCO Category 1 Institute

Effects of swift heavy ion irradiation and simulation of fission fragment impact

V.A.Skuratov

Flerov Laboratory of Nuclear Reactions
Joint Institute for Nuclear Research, Dubna, Russia

Press Release 30.05.2012 21:27

Element 114 is Named Flerovium and Element 116 is Named Livermorium

IUPAC

International Union of Pure and Applied Chemistry

IUPAC has officially approved the name flerovium, with symbol Fl, for the element of atomic number 114 and the name livermorium, with symbol Lv, for the element of atomic number 116.

Priority for the discovery of these elements was assigned to the collaboration between the Joint Institute for Nuclear Research (Dubna, Russia) and the Lawrence Livermore National Laboratory (Livermore, California, USA).

The name flerovium will honor the Flerov Laboratory of Nuclear Reactions where superheavy elements are synthesised. Georgiy N. Flerov (1913 – 1990) – was a renowned physicist, author of the discovery of the spontaneous fission of uranium, pioneer in heavy-ion physics, and founder in the Joint Institute for Nuclear Research the Laboratory of Nuclear Reactions (1957).

The name livermorium honors the Lawrence Livermore National Laboratory. A group of researchers of this Laboratory with the heavy element research group of the Flerov Laboratory of Nuclear Reactions took part in the work carried out in Dubna on the synthesis of superheavy elements including element 116.

Dubna: the root – “dub” – oak tree

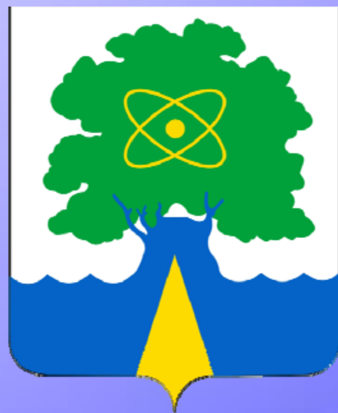

Swift heavy ions – ions with energies near and above 1 MeV/nucleon

Main sources of high energy ions:

I. **Accelerators**
II. **Galactic cosmic rays**
III. **Fission fragments**

I. Accelerators

High energy heavy ion accelerator facilities:

GANIL (Caen, France) 1-100 MeV/amu
GSI (Darmstadt, Germany) 10-1000 MeV/amu
NSC (New Delhi, India) 15 MeV×Z
JINR (Dubna, Russia) 1.2-10 MeV/amu
CRC (Louvain-la-Neuve, Belgium) 0.6-27.5 MeV/amu
ANU (Canberra, Austarlia) 15.5 MeV×Z
RIKEN (Tokai, Japan) 7-135 MeV/amu
JAERI (Takasaki, Japan) 2.5-90 MeV/amu
IRC (Astana, Kazakhstan) 0.42-1.67 MeV/amu
BNL (Berkeley, USA) 4.5-55 MeV/amu

Accelerator for applied research – IC100

B^{+2}, Ne^{+4}, Ar^{+7}, Kr^{+17}, Xe^{+26} ions with energy ≈ 1.2 MeV/amu

Ion fluence range – up to 10^{16} cm^{-2}

IC-100 cyclotron for applied research

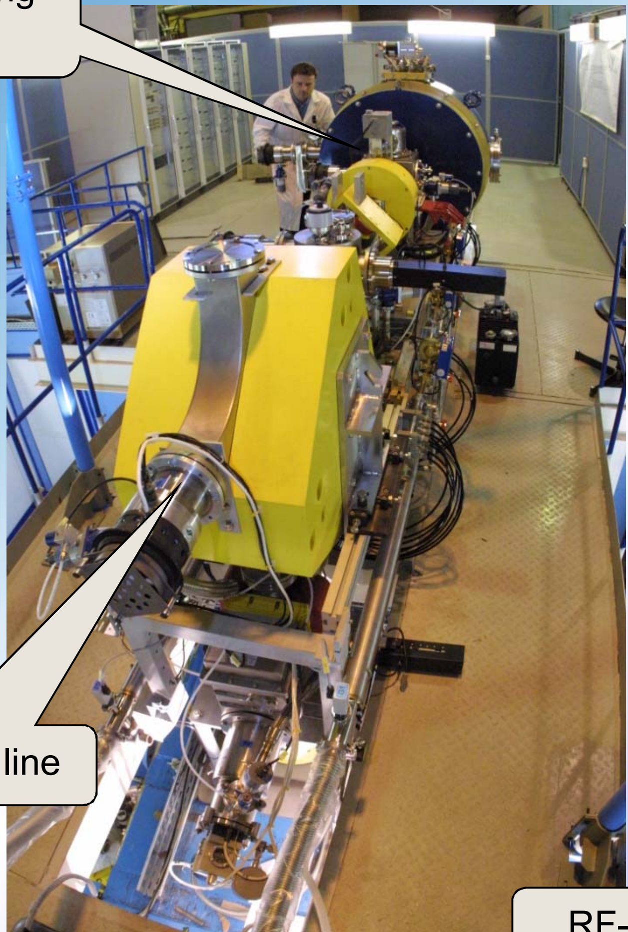

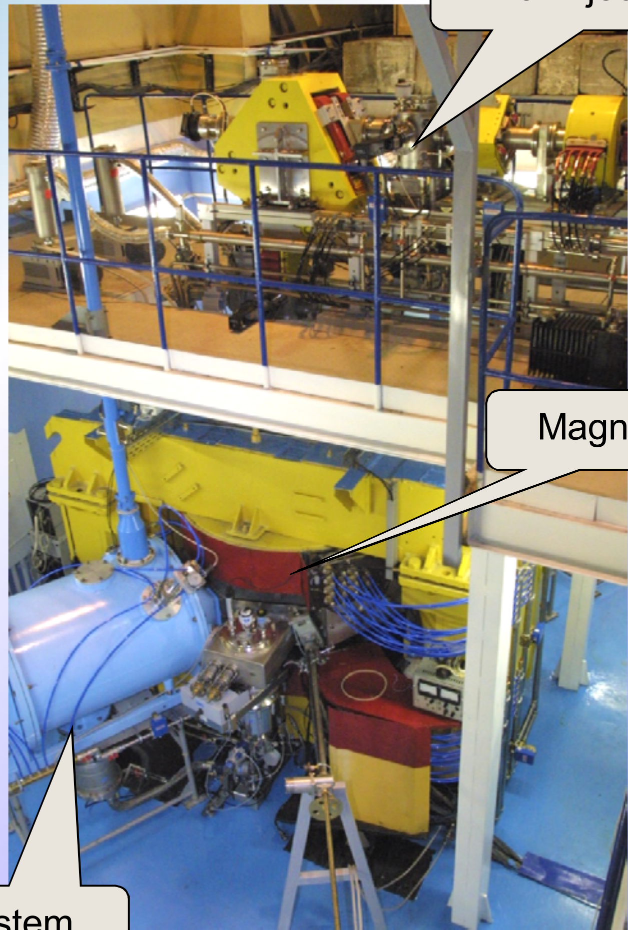

U400M FLNR JINR Cyclotron

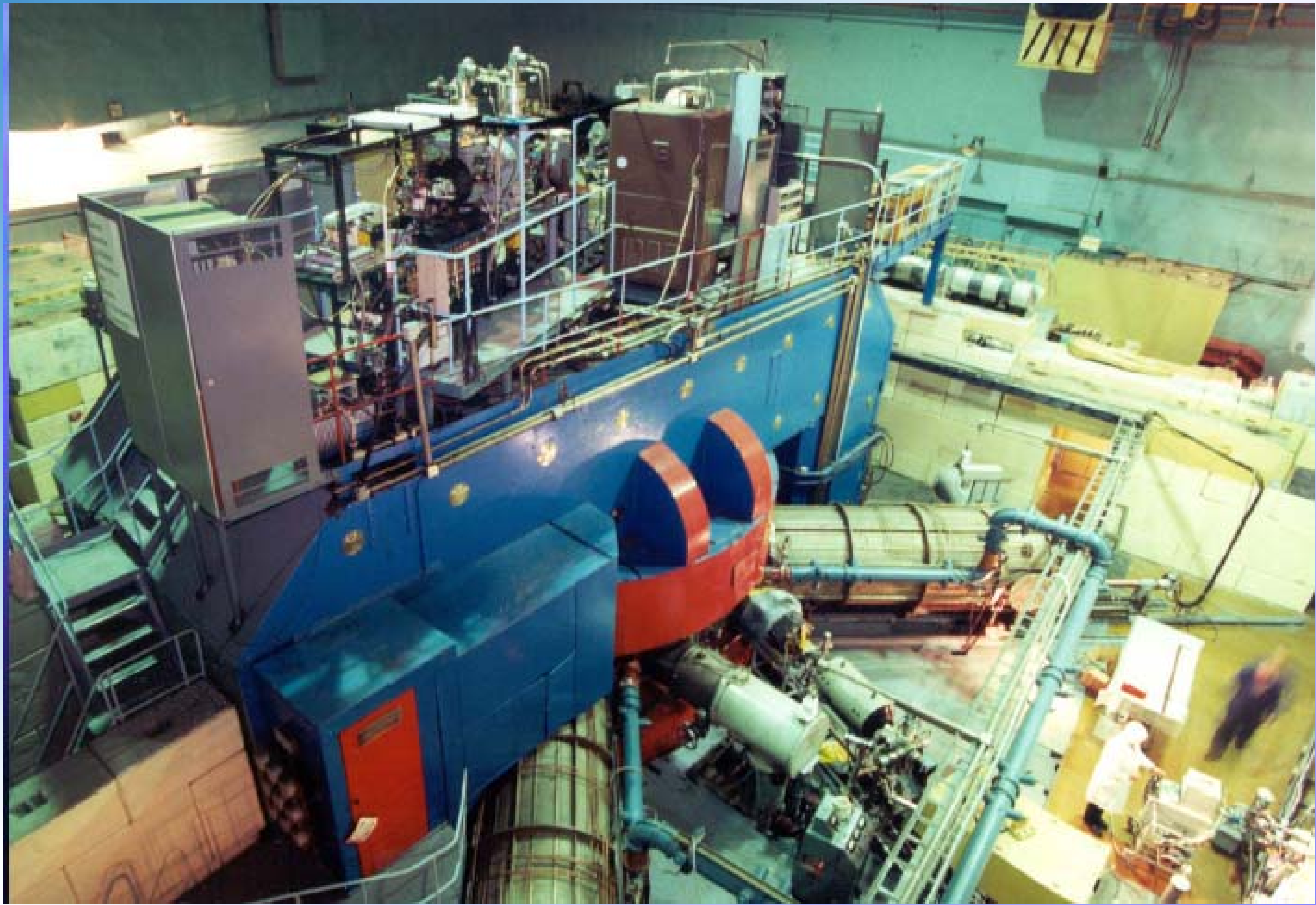

Ion Beam Line for SEE Testing at U400M FLNR JINR Cyclotron

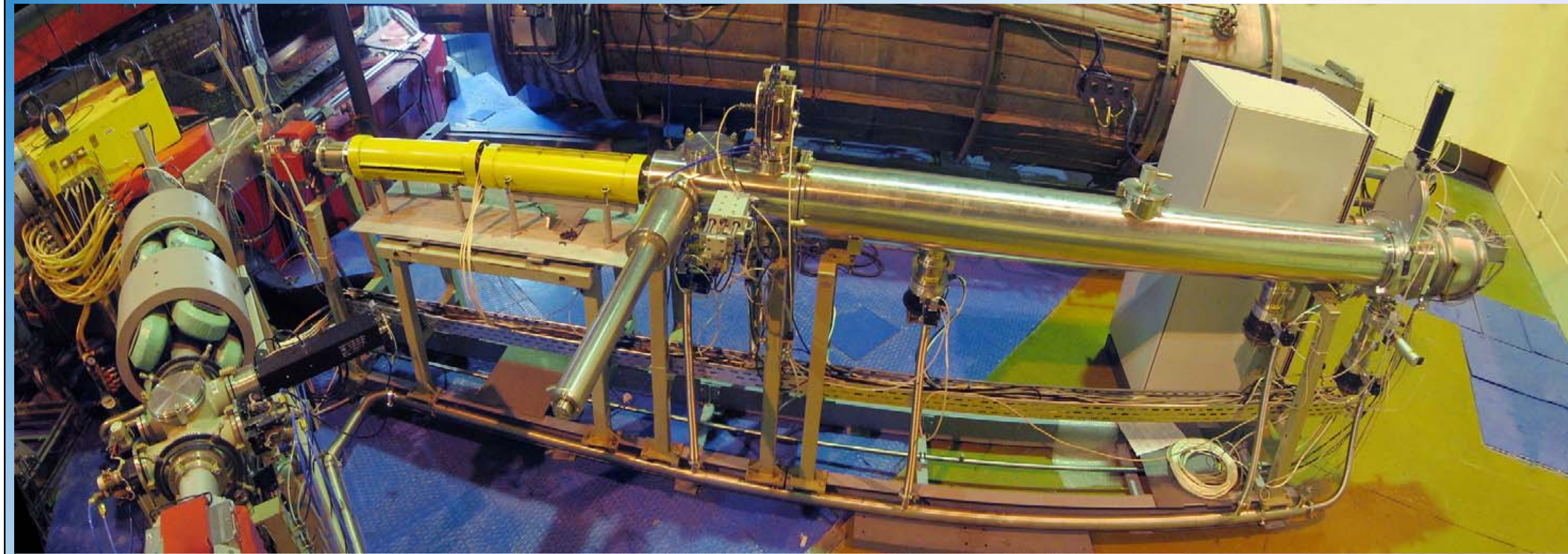

Ions $^{16}O \div {}^{209}Bi$, E= 3 ÷ 9 MeV/nucleon, LET = 4 ÷ 100 MeV/(mg/cm^2)

DC-60 CYCLOTRON (Astana)

E= 0.42-1.67 MeV/amu

II. Galactic cosmic rays

The composition of galactic cosmic rays includes:
83% protons
13% alpha particles
3% electrons
1% heavy ions (Z>4)

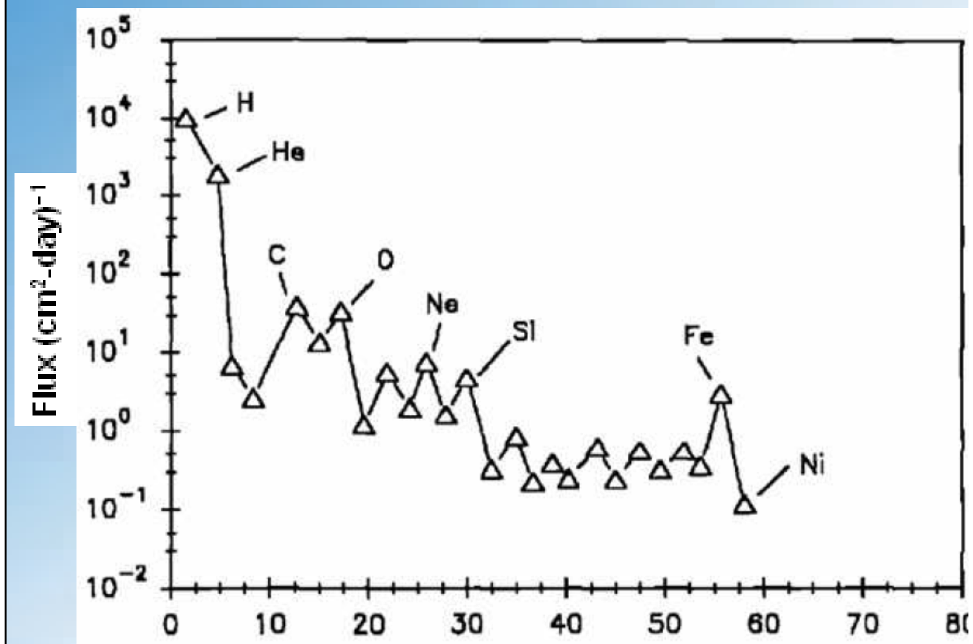

Nuclear charge (Z)

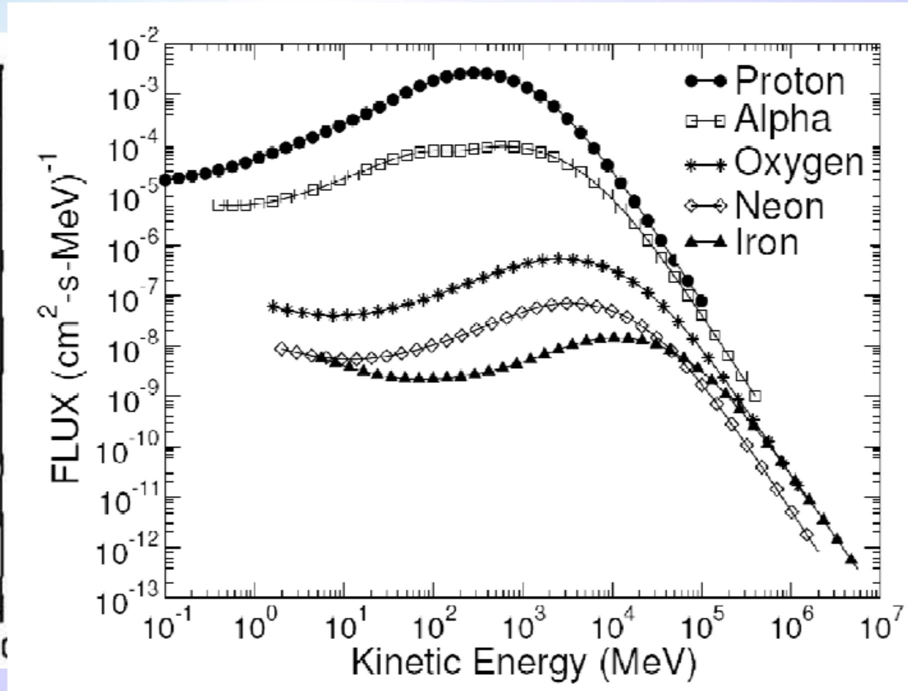

III. Fission fragments

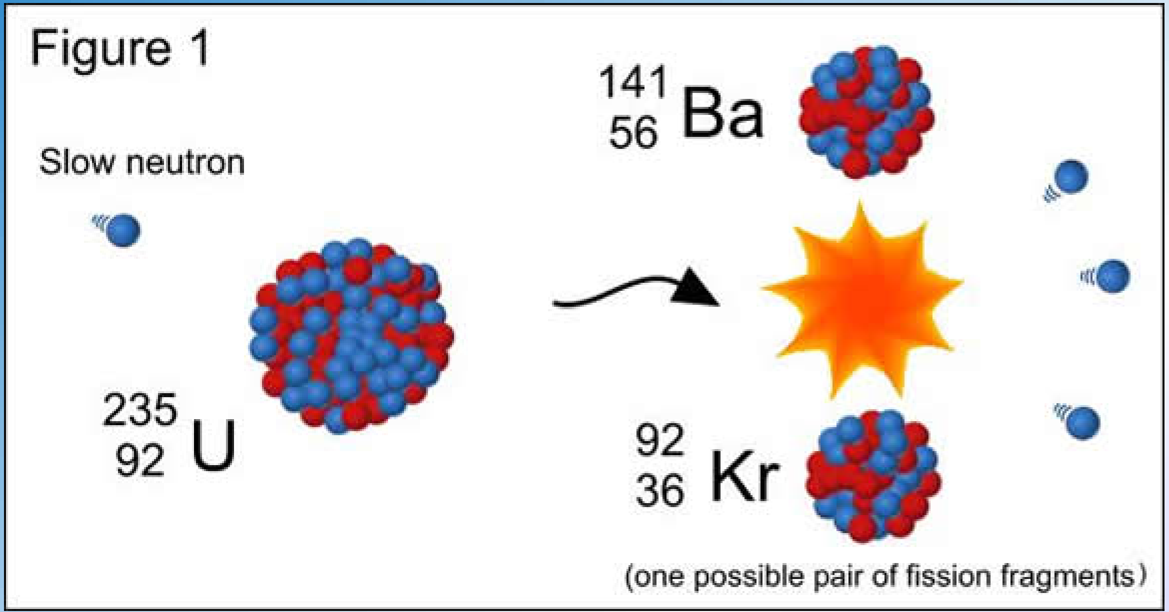

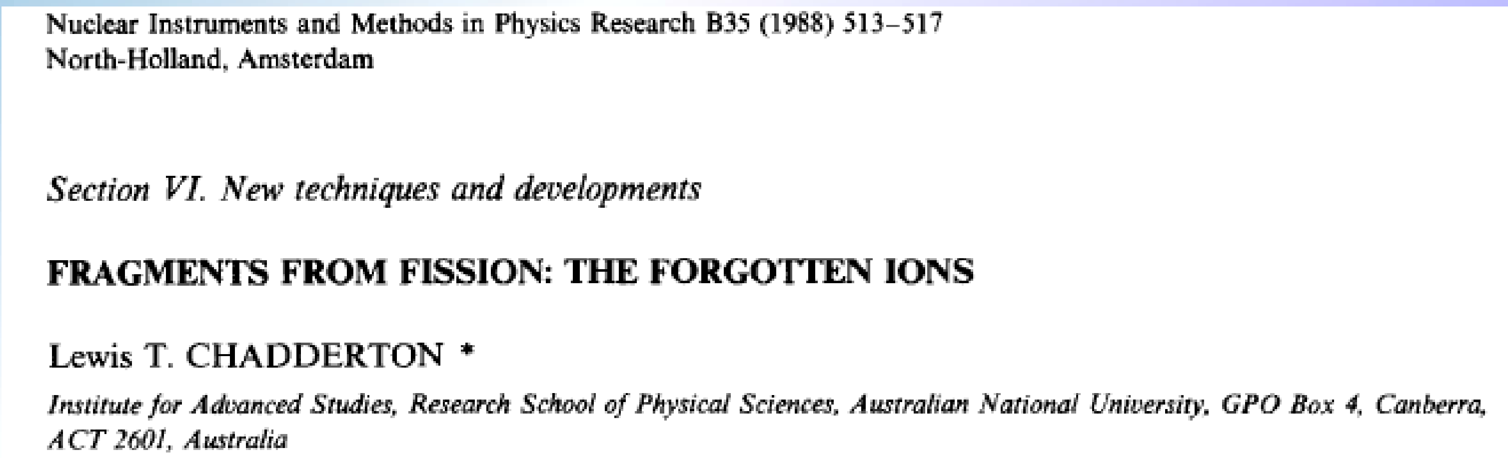

Nuclear Instruments and Methods in Physics Research B35 (1988) 513–517
North-Holland, Amsterdam

Section VI. New techniques and developments

FRAGMENTS FROM FISSION: THE FORGOTTEN IONS

Lewis T. CHADDERTON *

Institute for Advanced Studies, Research School of Physical Sciences, Australian National University, GPO Box 4, Canberra, ACT 2601, Australia

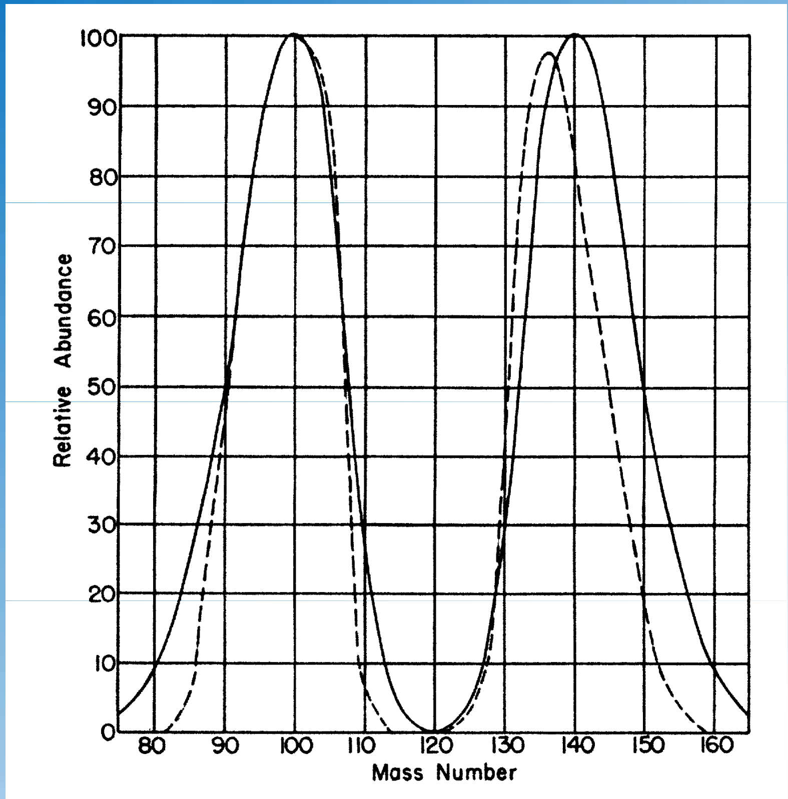

Mass distribution of fission fragments from Pu^{239}.
Solid line is coincident fragment experiment; dashed line is chemical analysis.
D.C.Brunton and W.B.Thomson. Phys. Rev. 76(1949), 848

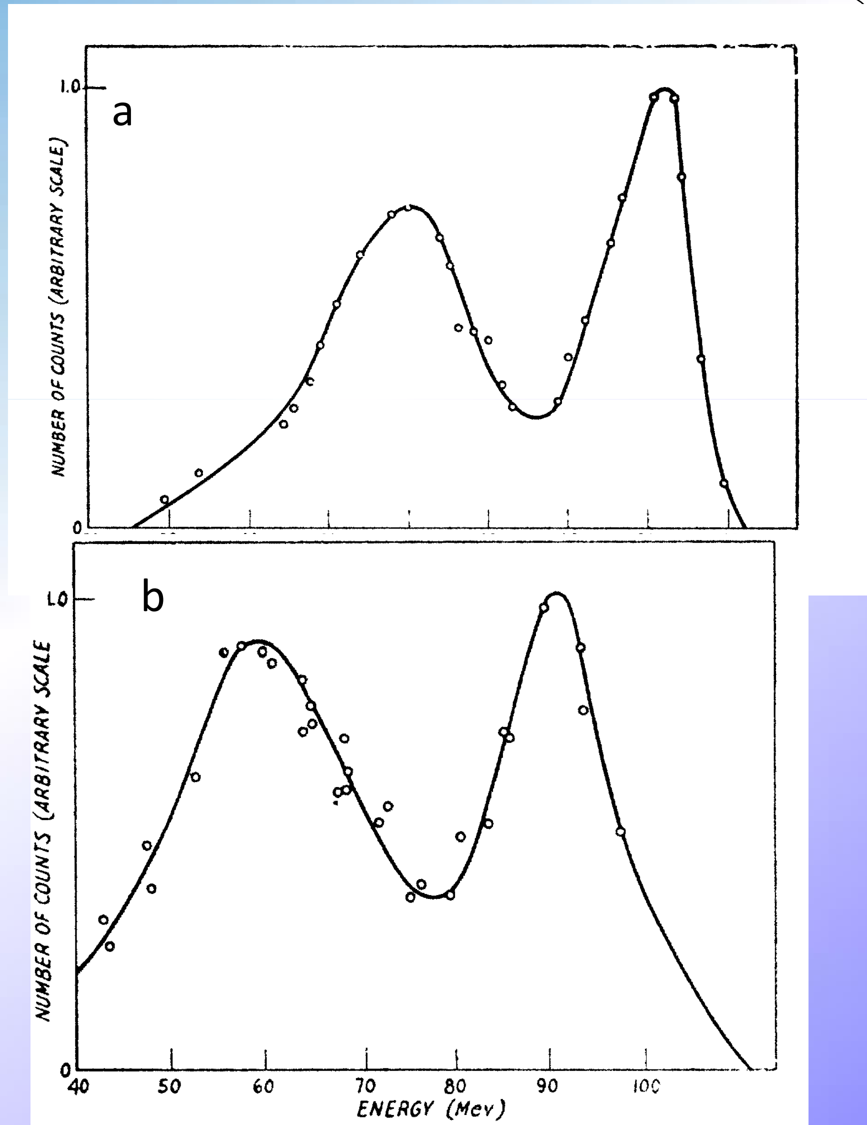

Energy spectrum of U^{235} fission fragments induced by thermal (a) and 2.5 MeV (b) neutrons.
Stephen S. Friedland. Phys. Rev. 84(1951), 75

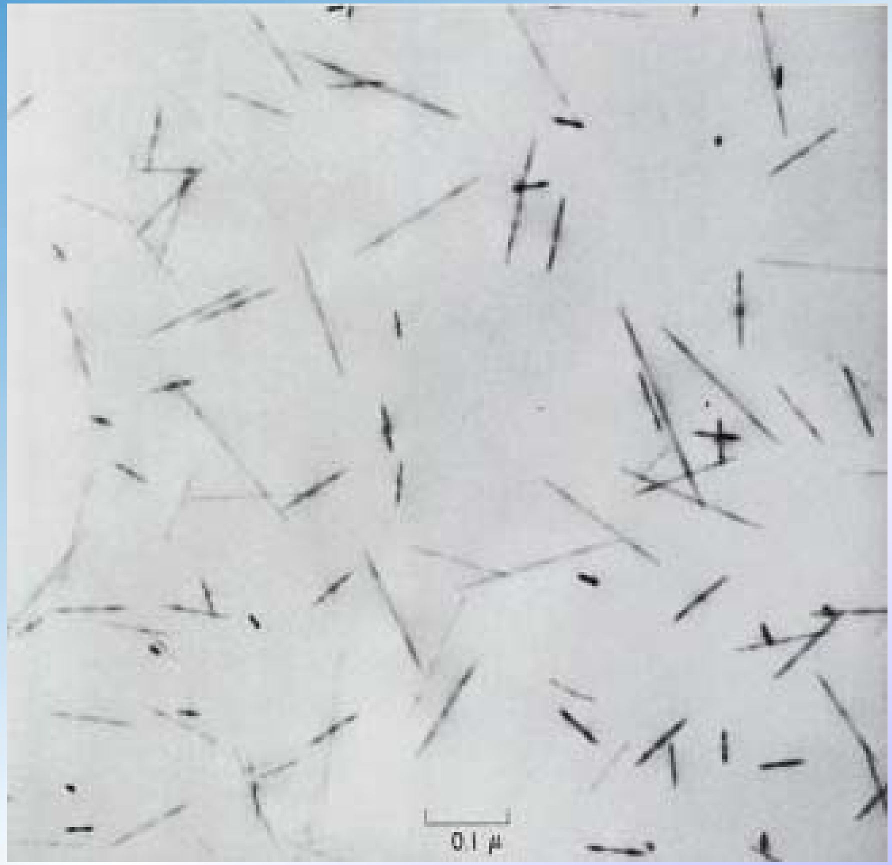

TEM image of tracks from ^{235}U fission fragments in a synthetic fluor-phlogopite mica.
R.L., P.B. Price, R.M. Walker: "Nuclear Tracks in Solids: Principles and Applications." University of California, Berkeley, 1-605, (1975)

Main peculiarity of swift heavy ion interaction with solids is a high level of ionizing energy losses which may result in formation of specific radiation damage – latent tracks

$$(-dE/dx)_{total} = (-dE/dx)_{electron} + (-dE/dx)_{nuclear}$$

$$\sim 99\% \qquad\qquad \sim 1\%$$

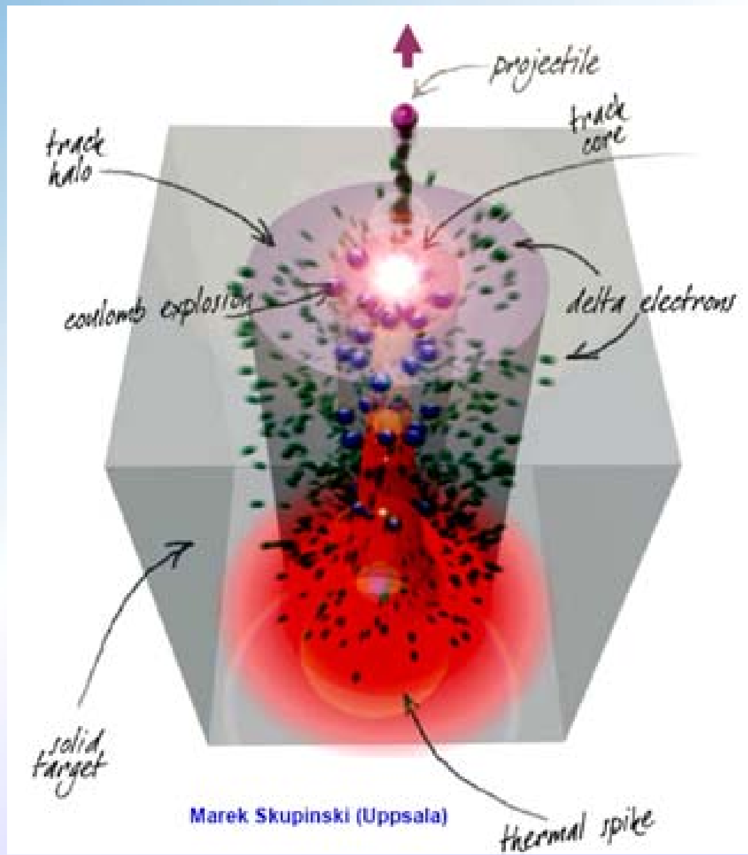

Aim of presentation – to give a review on structural effects of dense ionization in some nuclear ceramics and oxides under swift heavy ion irradiation simulating fission fragment impact

Materials to be considered – candidate materials for inert matrix fuel hosts (IMF)

Inert matrices - ceramics with a high melting point and with low neutron absorption cross sections to be used as hosts for transmutation of actinides via nuclear reactions

Ceramics and oxides considered as candidates for inert matrix fuel hosts - $MgAl_2O_4$, MgO, Al_2O_3, ZrO_2, SiC, ZrC, ZrN, AlN, Si_3N_4

Examples of fuel compositions for LWR:

$(Pu)O_2$ - MgO-ZrO_2

$(Pu,Np,Am)O_2$, MgO-ZrO_2

$(Am,Np,Pu,Zr)N$

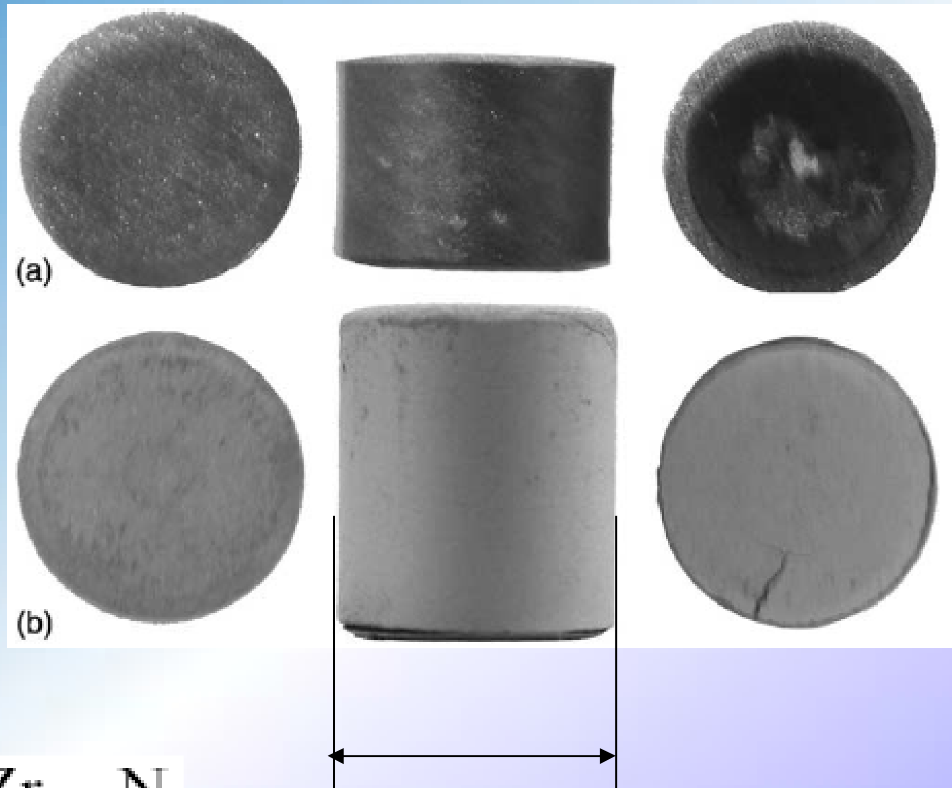

8,2 мм

$Pu_{0.25}Zr_{0.75}N$

M. Streit et al. Journal of Nuclear Materials 319 (2003), pp. 51–58

Phase transformations and accompanying volume changes in swift ion/(fission fragment track region may produce unacceptable stresses in fuel pin assemblies

Al_2O_3: $\rho_{crystalline}/\ \rho_{amorphous} = 0.03$

Our central objectives are:
- Threshold electron stopping power for radiation damage formation via electronic excitations - ?
- single ion track and ion track overlapping irradiation regimes- ?
- dense ionization effect on pre-existing defect structure in irradiating materials - ?
- correlation between surface and material bulk radiation damage induced by heavy ions with energies above 1 MeV/amu - ?
- evaluation of mechanical stresses in oxides - ?

Examination of the dense ionization effect in ceramics and oxides with heavy ions of fission fragments energy

$MgAl_2O_4$

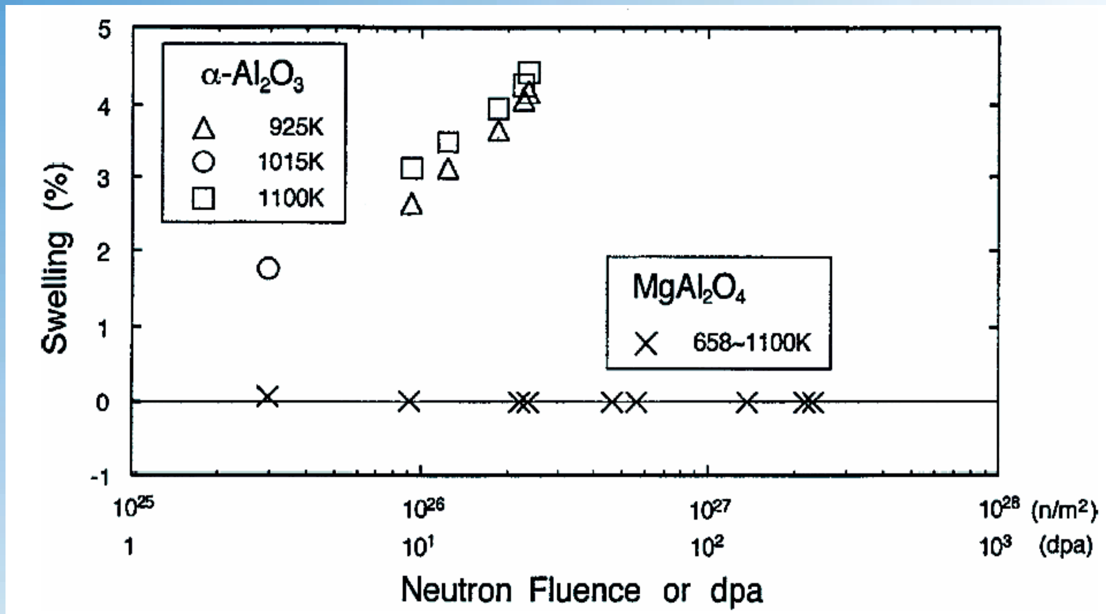

C. Kinoshita. Microstructural evolution of irradiated ceramics. In: Radiation effects in solids. Eds. K.Sickafus, E.Kotomin and B.Uberaga. Nato Science series. V.232, p.193

spinel is not amorphized by electron, neutron and low-energy ion irradiation at T > 300 K

Examination of the dense ionization effect in ceramics and oxides with heavy ions of fission fragments energy

$MgAl_2O_4$

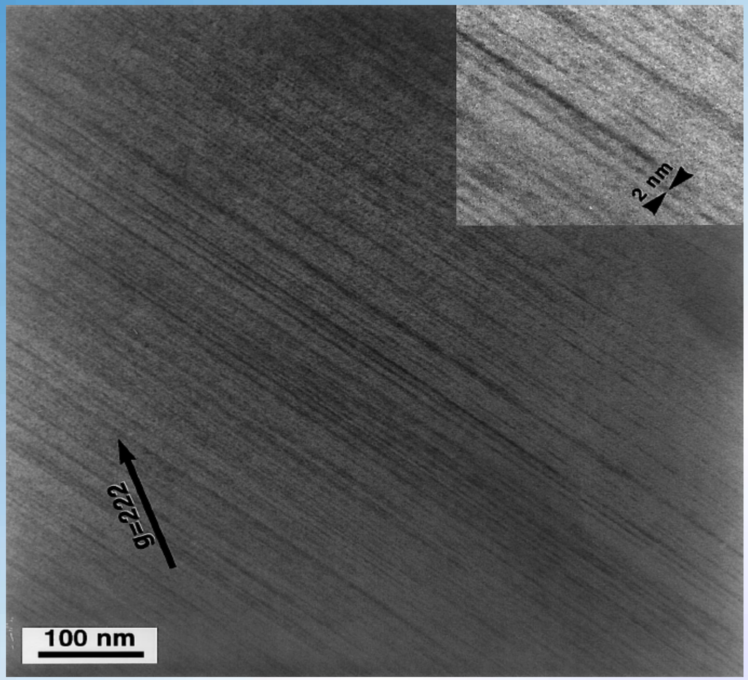

Ion tracks in spinel irradiated with 430 MeV Kr ions to a fluence of 1.1×10^{12} cm^{-2} at room temperature.

The average TEM **track diameter is ~2 nm**.

S.J. Zinkle, V.A. Skuratov . NIMB. B 141 (1998) 737

Examination of the dense ionization effect in ceramics and oxides with heavy ions of fission fragments energy

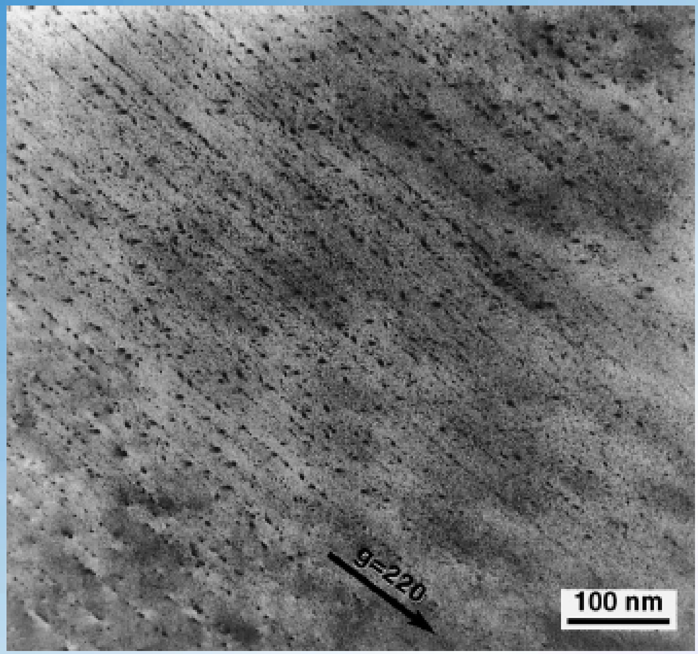

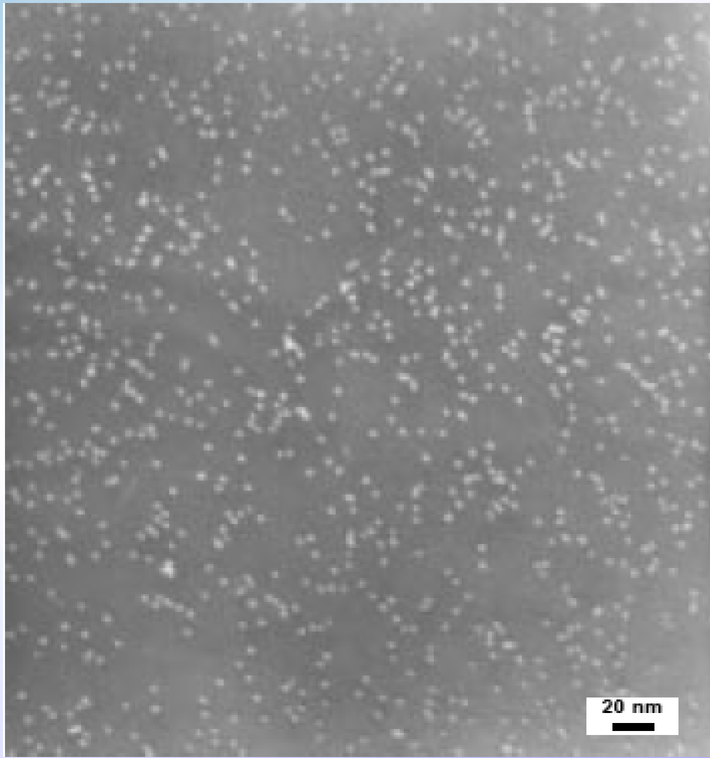

Ion tracks in spinel irradiated with 430 MeV Kr ions

Swift heavy ions induce discontinuous nonamorphous tracks

S.J. Zinkle, V.A. Skuratov . NIMB. B 141 (1998) 737

Examination of the dense ionization effect in ceramics and oxides with heavy ions of fission fragments energy

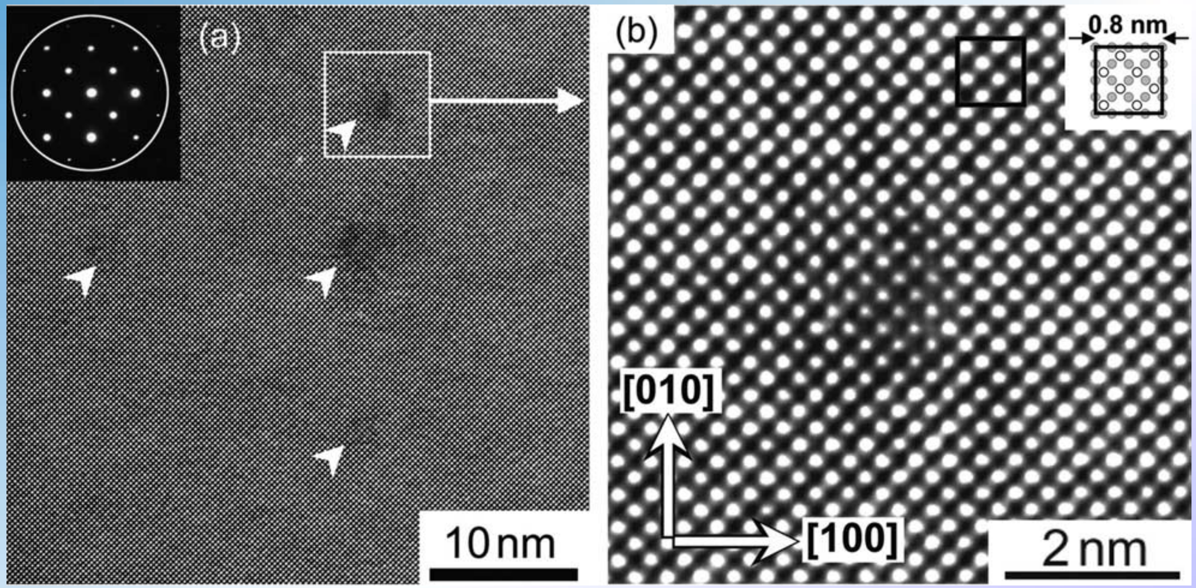

HR lattice images of spinel irradiated with 5 ×10^{11} 200 MeV Xe ions/cm^2

T. Yamamoto et al. / Nucl. Instr. and Meth. in Phys. Res. B 245 (2006) 235–238

Examination of the dense ionization effect in ceramics and oxides with heavy ions of fission fragments energy

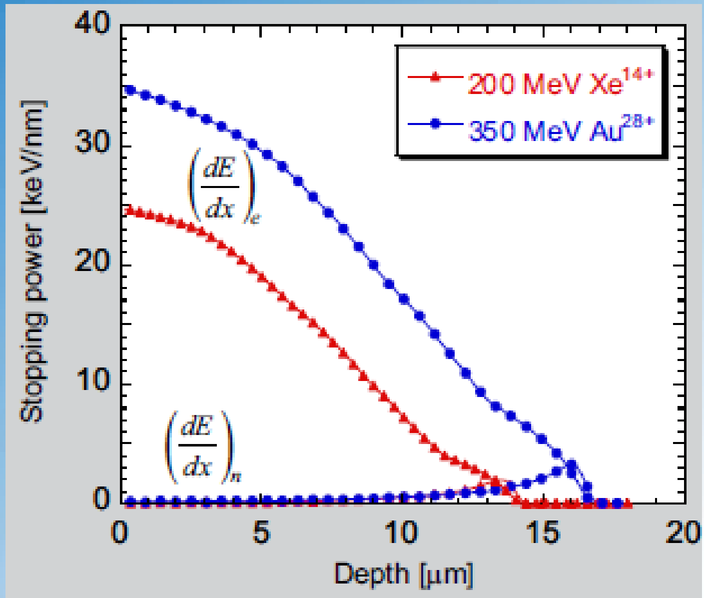

The calculated electronic and nuclear stopping power profiles in $MgO \cdot 1.1Al_2O_3$ irradiated with 200 MeV Xe and 350 MeV Au ions

Track core size : 2-3 nm
Strained regions size: (around 5 nm)

The size of the disordered regions

Xe, 200 MeV	**Au, 350 MeV**
12.8±0.9 nm for Al ions	10.6±0.7 nm for Al ions
9.6±0.4nm for Mg ions	8.8±0.5 nm Mg ions

The disordered regions are around 10 nm in diameter

K. Yasuda, T. Yamamoto and S. Matsumura. JOM Journal of the Minerals, Metals and Materials Society 59(2007), N4, 27.

Examination of the dense ionization effect in ceramics and oxides with heavy ions of fission fragments energy

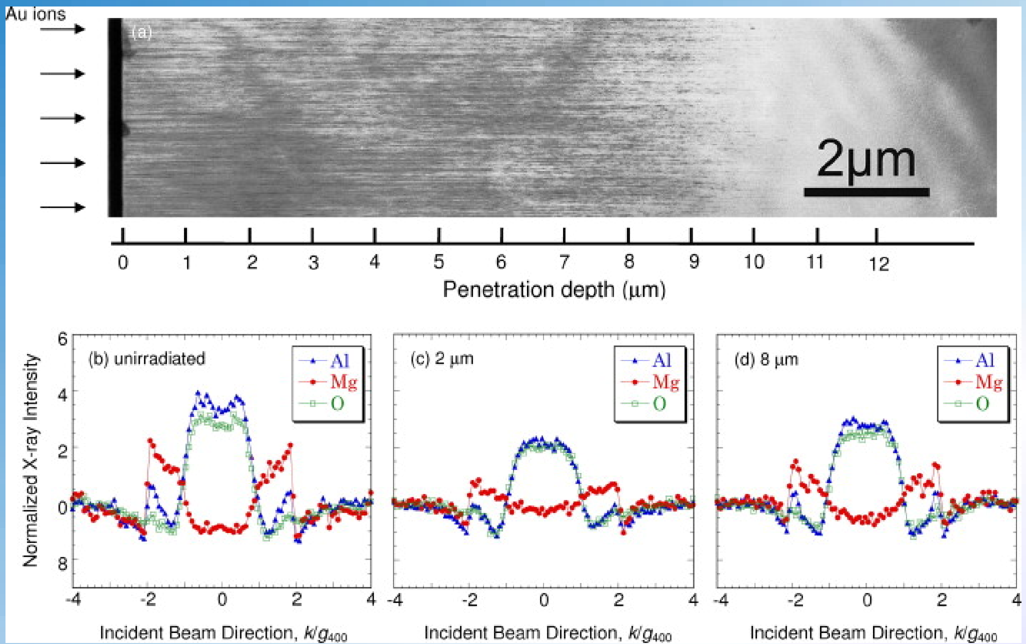

Bright-field cross section view of $MgO \cdot 1.1Al_2O_3$, illustrating continuous ion tracks along incident ions (a), irradiated at 300 K with 350 MeV Au ions to a fluence of 5×10^{11} ions/cm^2, and HARECXS profiles taken from an unirradiated specimen (b) and from a depth of 2 μm in the irradiated specimen (c) and from a depth of 8 μm (d).

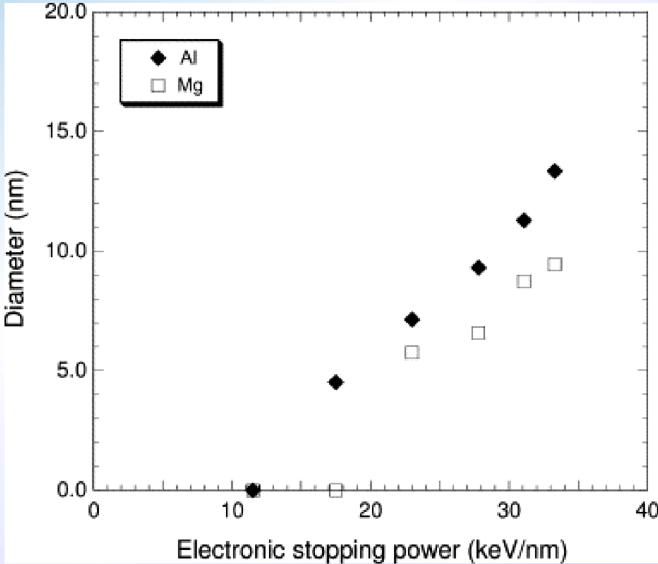

Diameter of the disordered region induced by one 350 MeV Au ion in $MgO \cdot 1.1Al_2O_3$ as a function of electronic stopping power

K. Yasuda et al. / NIM B 266 (2008) 2834–2841

Examination of the dense ionization effect in ceramics and oxides with heavy ions of fission fragments energy

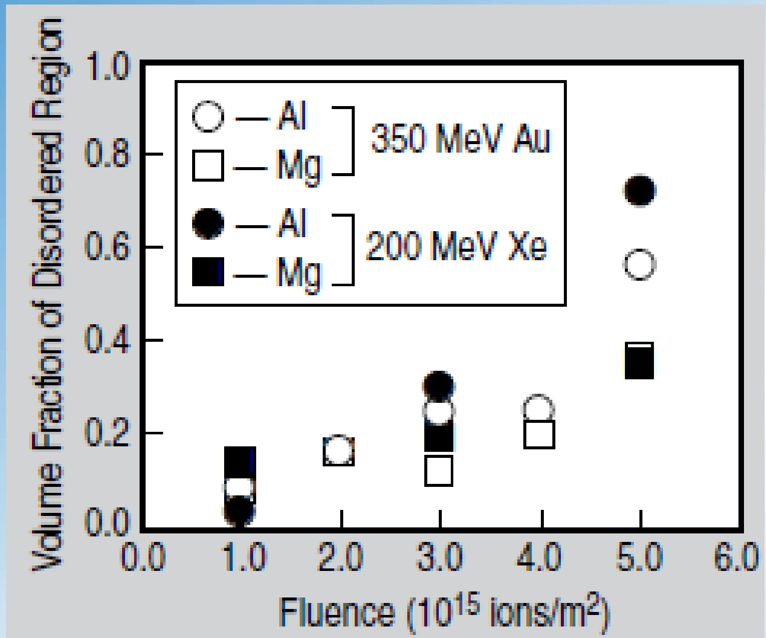

The volume fraction of disordered damage region of MgO $\cdot 1.1 Al_2O_3$ irradiated with 200 MeV xenon and 350 MeV gold ions against of ion fluence.

K. Yasuda, T. Yamamoto and S. Matsumura. JOM Journal of the Minerals, Metals and Materials Society 59(2007), N4, 27.

Examination of the dense ionization effect in ceramics and oxides with heavy ions of fission fragments energy

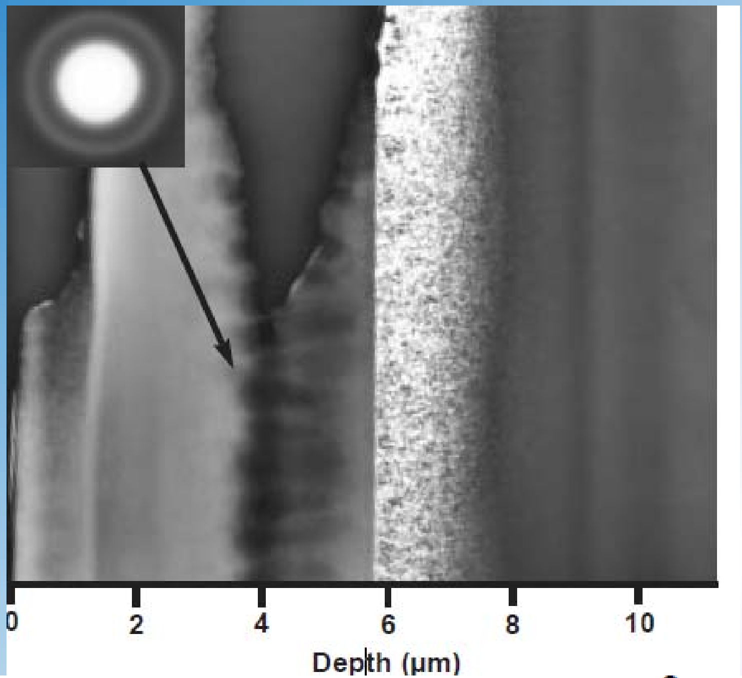

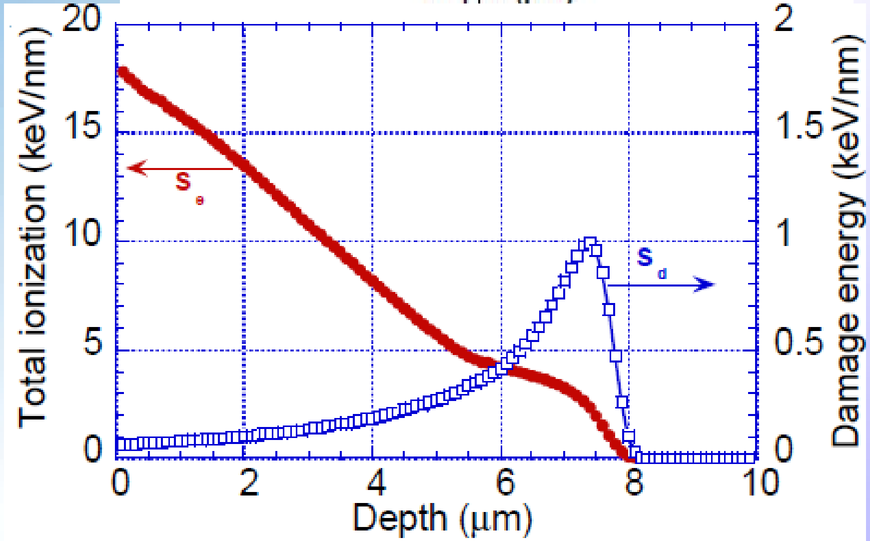

Cross-section microstructure of $MgAl_2O_4$ irradiated to a fluence of 1×10^{16} 72 MeV Iodine ions/cm^2

volumetric swelling is ≈35% for the crystalline to amorphous phase transformation

Heavy ions of fission products energy can amorphize spinel. Ion fluence threshold for amorphization is between 1×10^{13} and 5 1×10^{13} cm^{-2}

Ion track region area for R=1 nm =10^{-7} cm
S = 3.14× 10^{-14} cm^2
Ion fluence needed to cover area 1 cm^2
$\Phi = 1/3.14 \times 10^{-14}$ cm^2 ≈ 3.18×10^{13} cm^{-2}
R=2 nm, $\Phi = 1/12.56 \times 10^{-14}$ cm^2 ≈ 7.9×10^{12} cm^{-2}

Proc. 540 (1999) 299.

Examination of the dense ionization effect in ceramics and oxides with heavy ions of fission fragments energy

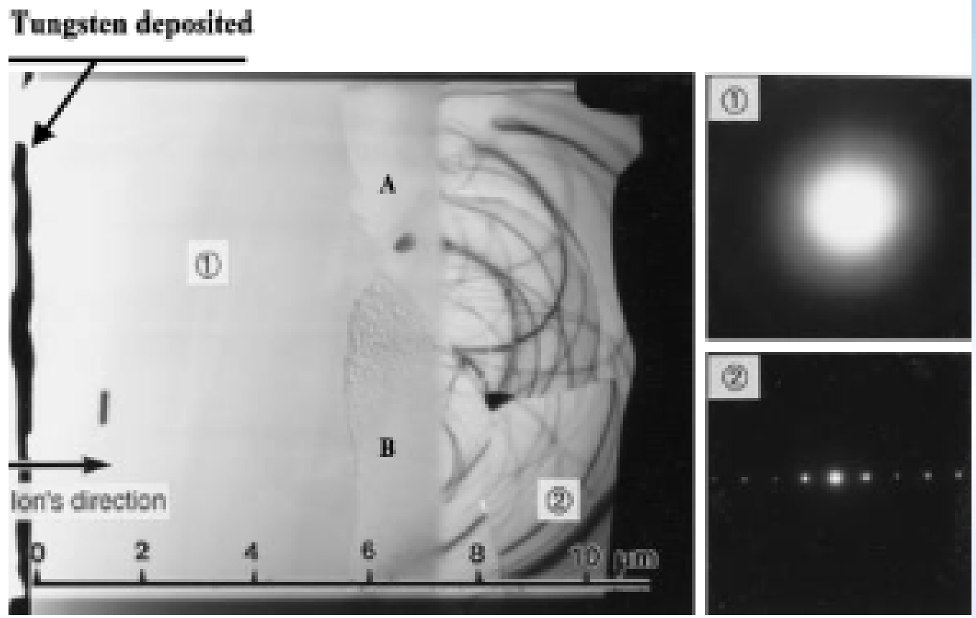

XTEM image of polycrystalline $MgAl_2O_4$ sample irradiated with 85 MeV I^{+7} ions to 1.2×10^{15} cm^{-2}

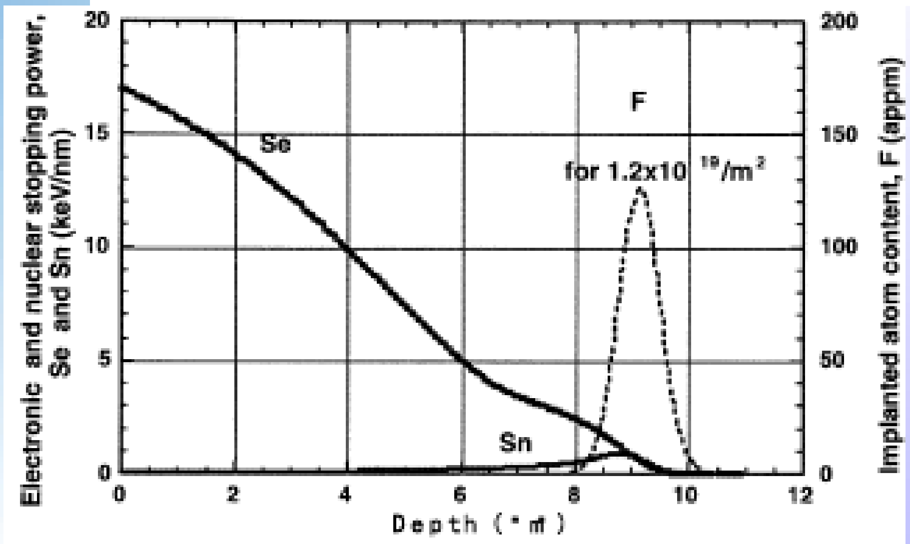

Electronic and nuclear stopping powers, Se, Sn of $MgAl_2O_4$ for incident 85 MeV I^{+7} ions as a function of depth. Ion fluence 1.2×10^{15} cm^{-2}

T. Aruga et al. / NIM B 197 (2002) 94–100

Examination of the dense ionization effect in ceramics and oxides with heavy ions of fission fragments energy

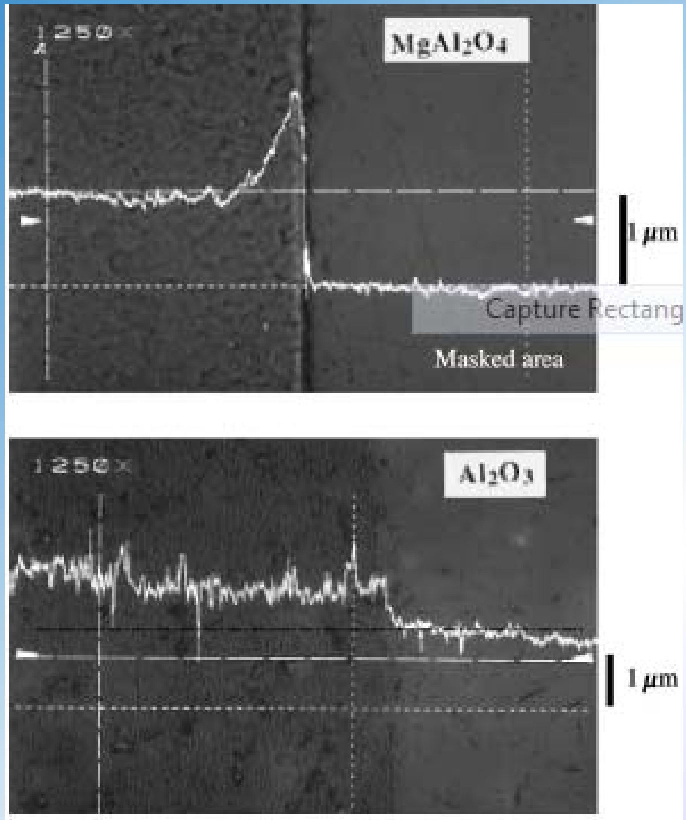

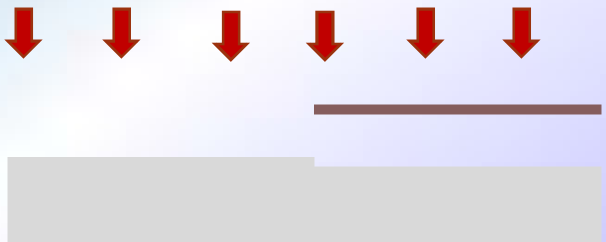

Step heights formed on the surfaces of $MgAl_2O_4$ and Al_2O_3 along a border of masked and 85 MeV I^{+7} ion irradiated area. Ion fluence 1.2×10^{15} cm-^{2}

The swelling due to amorphization is estimated to be around 15–20%

T. Aruga et al. / NIM B 197 (2002) 94–100

Examination of the dense ionization effect in ceramics and oxides with heavy ions of fission fragments energy

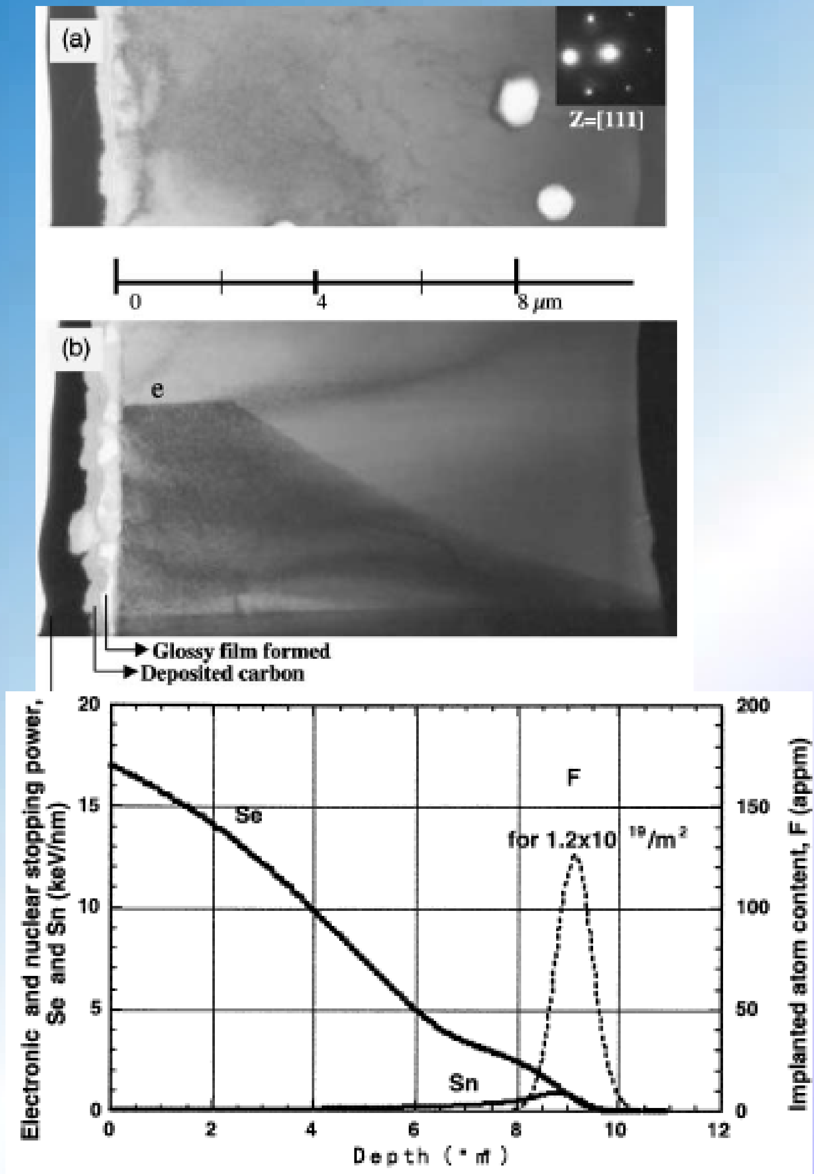

XTEM image of polycrystalline MgO sample irradiated with 85 MeV I^{+7} ions to 0.28×10^{15} cm^{-2} (a) and 1.2×10^{15} cm^{-2} (b)

No amorphization occurs for MgO samples at the fluence of 1.2×10^{15} cm^{-2}

T. Aruga et al. / NIM B 197 (2002) 94–100

Examination of the dense ionization effect in ceramics and oxides with heavy ions of fission fragments energy

Dense ionization effect on pre-existing defect structure in $MgAl_2O_4$

$MgAl_2O_4$ + 2 MeV Al , 950 K, 30-100 dpa
Defect structure – interstitial loops (Ø ~30 nm, N~ 4× 10^{15} см$^{-3}$), Al precipitates (2÷25 nm, N ~10^{15} см$^{-3}$)

$MgAl_2O_4$ + 3.6 MeV Fe , 950 K, 1-6 dpa
Defect structure – interstitial loops (Ø ~5 nm, N ~2×10^{17} см$^{-3}$)

the loop size had decreased to 4 nm and the loop density had increased to N ~4×10^{17} см$^{-3}$

+ 430 MeV Kr
1.1×10^{12} cm^{-2}

Swift heavy ion irradiation induces dissolution of dislocation loops which size is comparable with latent track diameter

S.J. Zinkle, V.A. Skuratov . Nucl. Instr. and Meth.. B 141 (1998) 737

Examination of the dense ionization effect in ceramics and oxides with heavy ions of fission fragments energy

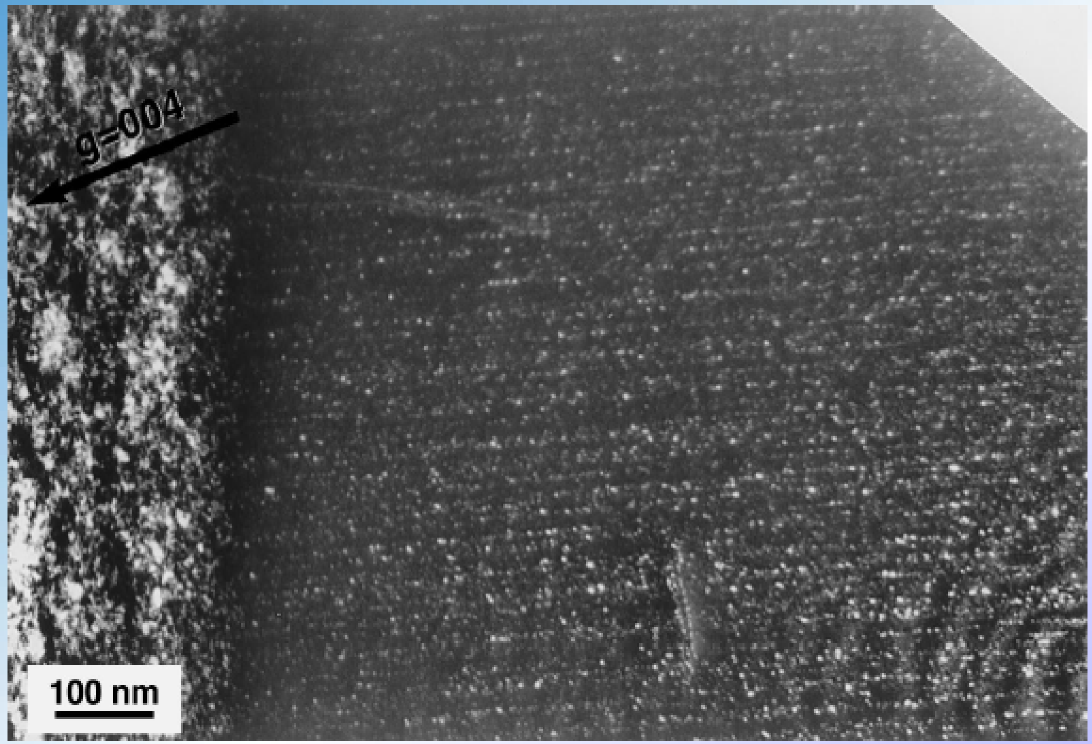

Microstructure beyond the end of range of the 2 MeV Al ion pre-irradiated region in spinel after 430 MeV Kr ion irradiation

S.J. Zinkle, V.A. Skuratov . Nucl. Instr. and Meth.. B 141 (1998) 737

Examination of the dense ionization effect in ceramics and oxides with heavy ions of fission fragments energy

Summary on $MgAl_2O_4$:

Threshold ionizing radiation levels for track in spinel - 6 ÷ 8 keV/nm

Multiple overlapping of the ion track regions leads to amorphization of $MgAl_2O_4$

High energy heavy ion irradiation may induce dissolution of dislocation loops which size is comparable with latent track diameter

Ion	Energy, MeV	Fluence ions, cm^{-2}	dE/dx, keV nm^{-1}	Ref.	Swelling, %	Track radius, nm	Accelerator
^{127}I	70	10^{11}	16	this work		1.5	[1]TU Munich
^{127}I	70	10^{13}	16	"		Not observed	-
^{127}I	70	$5{\cdot}10^{12}$	16	"	0		"
^{127}I	70	$5{\cdot}10^{13}$	16	"	11.4 (7.25)*		"
^{127}I	70	$5{\cdot}10^{14}$	16	"	22.2 (13.5)*		"
^{127}I	70	$5{\cdot}10^{15}$	16	"	33.1 (21)*		"
^{209}Bi	120	$5{\cdot}10^{10}$	23	"		3.4	[2]GSI
^{209}Bi	2380	$5{\cdot}10^{10}$	34	"		1.7	GSI
^{238}U	2710	$5{\cdot}10^{10}$	41	"		1.5	GSI
^{86}Kr	430	$1.1{\cdot}10^{12}$	16	[13]		1	[3]U-400
^{129}Xe	614	6.10^{11}	26	[13]		1.3	U-400

[1] TANDEM of Beschleunigerlaboratorium der LMU und TU München,
[2] UNILAC of Gesellschaft für Schwerionenforschung, Darmstadt
[3] U-400 cyclotron of Joint Institute for Nuclear Research, Dubna.
* The swelling values in brackets are previously reported results [12] which were obtained using the ion full range.

T. Wiss et al. Progress in Nuclear Energy. Vol. 38, NO. 3-4, pp. 281-286, 2001

Examination of the dense ionization effect in ceramics and oxides with heavy ions of fission fragments energy

Al_2O_3

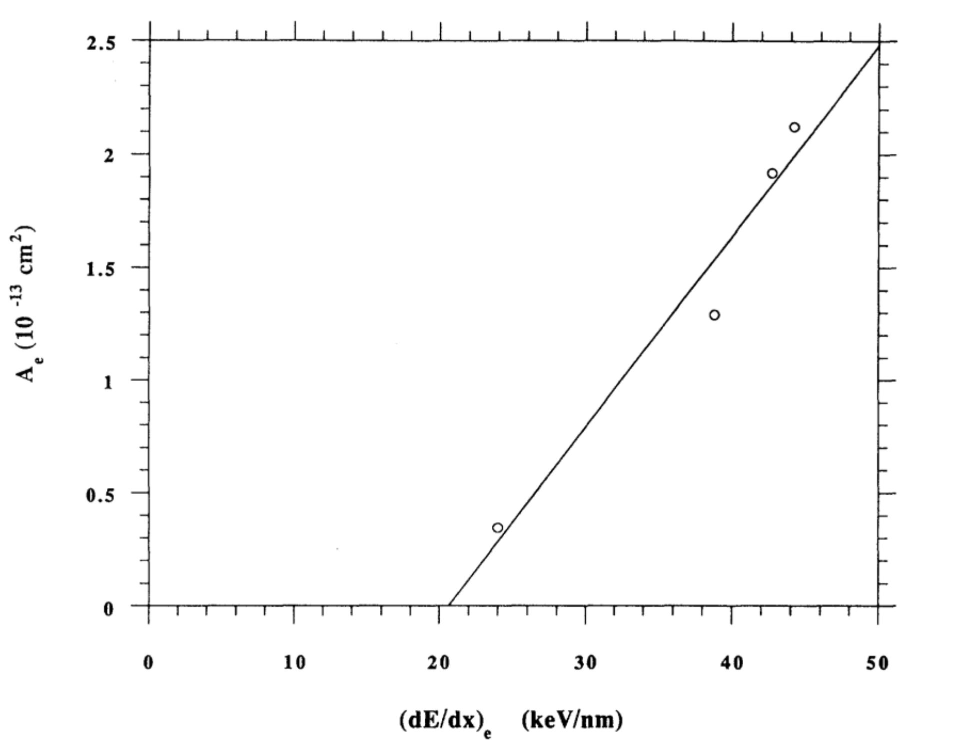

Evolution of the damage cross-section vs electronic stopping power Al_2O_3. The threshold of damage formation through dense ionization is about **20 keV/nm**

RBS-C analysis

α –relative disorder near the sample surface

$$\alpha = \frac{\chi_0 - \chi_v}{1 - \chi_v}$$

χ_0 – dechanneling yield

χ_0 - minimum yield

$$\alpha = 1 - \exp(-A_e \Phi)$$

***A*$_e$** – damage cross-section

B.Canut et al. PRB Vol. 51, No. 18, pp. 12194-12201, 1995

Examination of the dense ionization effect in ceramics and oxides with heavy ions of fission fragments energy

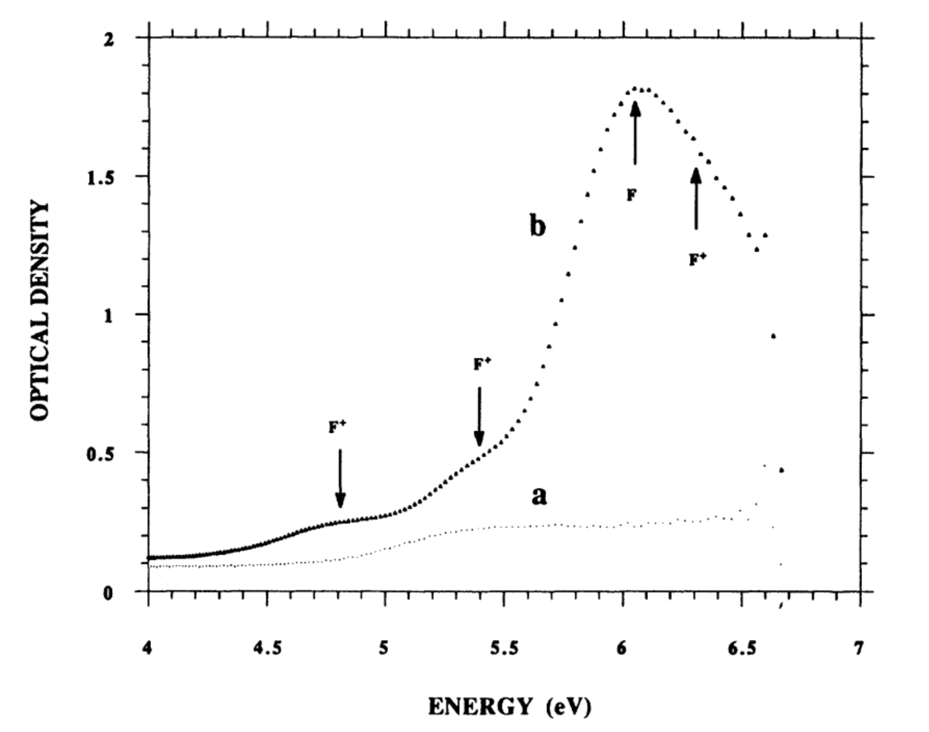

^{238}U (115 MeV, 2.46×10^{12} cm^{-2}) + α-Al_2O_3

The major part of F-type defects is created by elastic processes

Evaluation of the F-type defect concentration from optical absorption spectra

$$\mathbf{N = 1.31\times10^{16}(A\times W_{1/2})/f}$$

A -absorbance at peak position
$\mathbf{W_{1/2}}$ is the full width at the half maximum of the absorption peak (eV), **f** – oscillator strength

B.Canut et al. PRB Vol. 51, No. 18, pp. 12194-12201, 1995

Examination of the dense ionization effect in ceramics and oxides with heavy ions of fission fragments energy

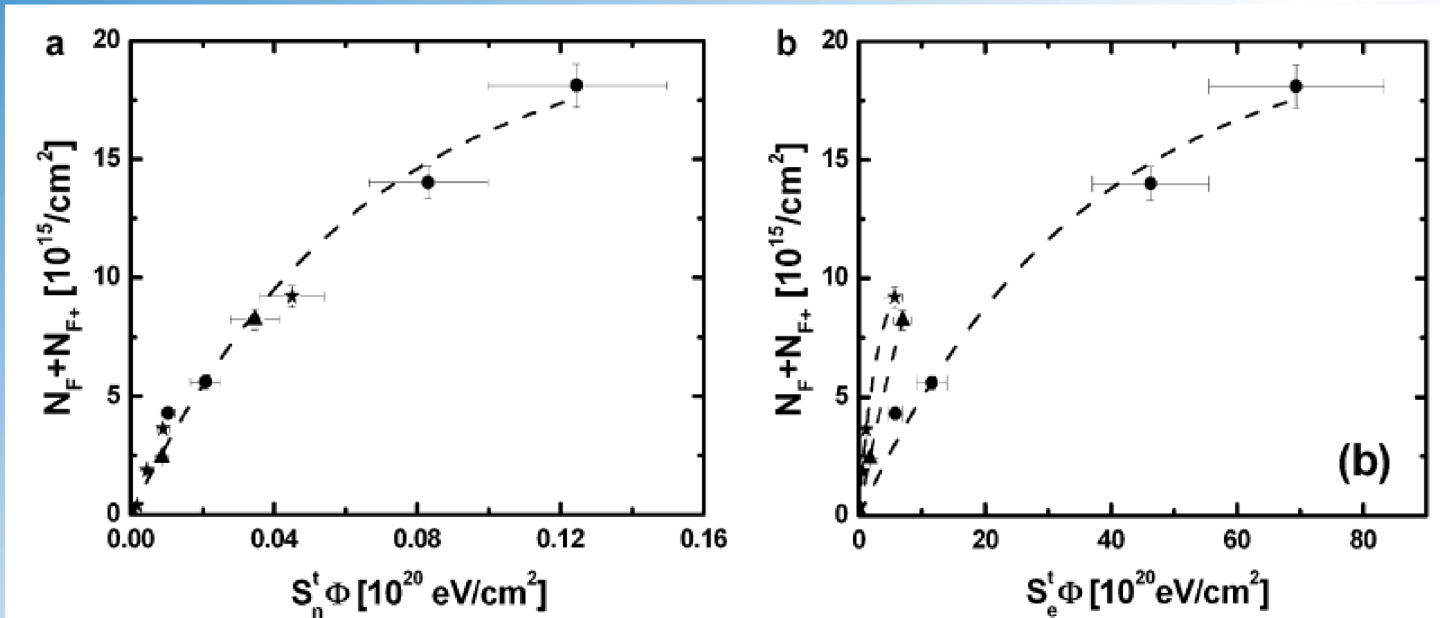

1.157 GeV ^{56}Fe (●), 1.755 GeV ^{136}Xe(▲), 2.636 GeV ^{238}U(★)

The nuclear energy loss processes determines the production of F-type defects in swift heavy ion irradiated Al_2O_3

Y. Song et al. / NIMB 254 (2007) 268–272

Mean positron lifetime vs. Ion fluence in irradiated sapphire

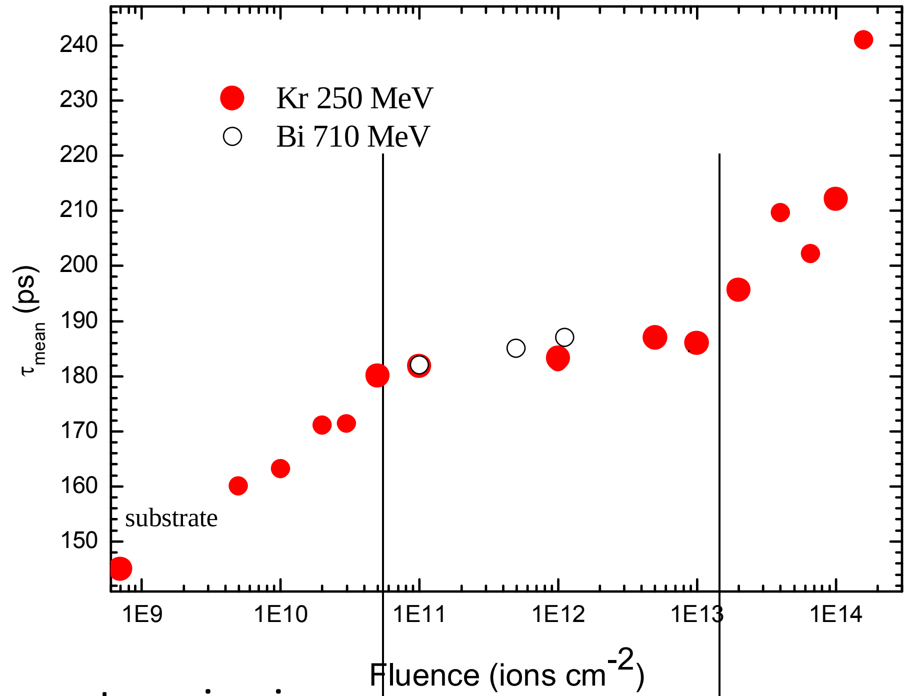

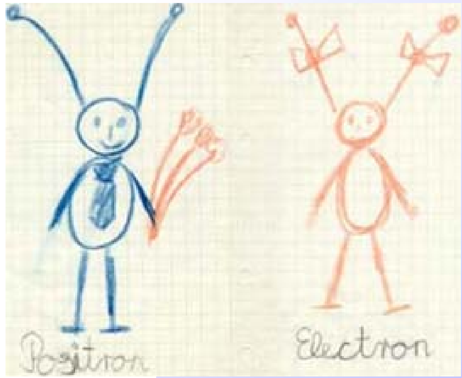

trapping in vacancies

saturated trapping in vacancies

trapping in larger defects

The figure shows different stages of point defect accumulation

Examination of the dense ionization effect in ceramics and oxides with heavy ions of fission fragments energy

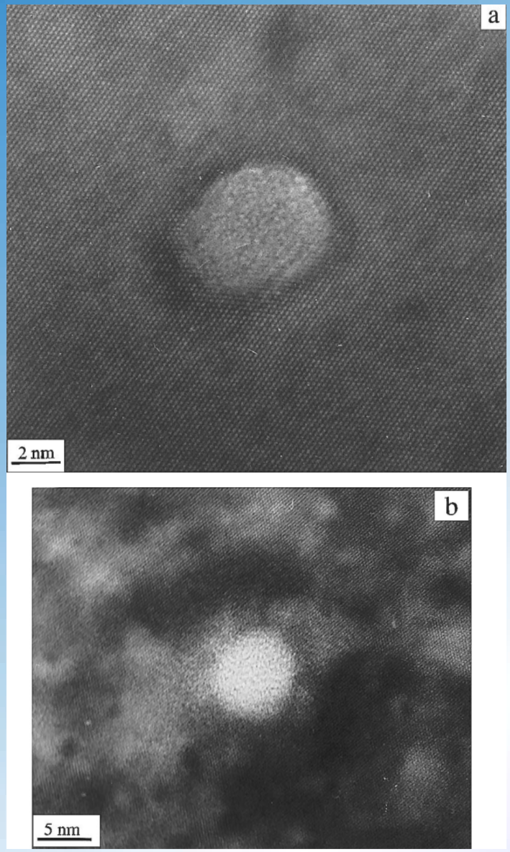

HREM micrograph of sapphire irradiated with 30 MeV $^{60}C^{2+}$ (a) and 10 MeV $^{60}C^{+}$ (b) at normal incidence.

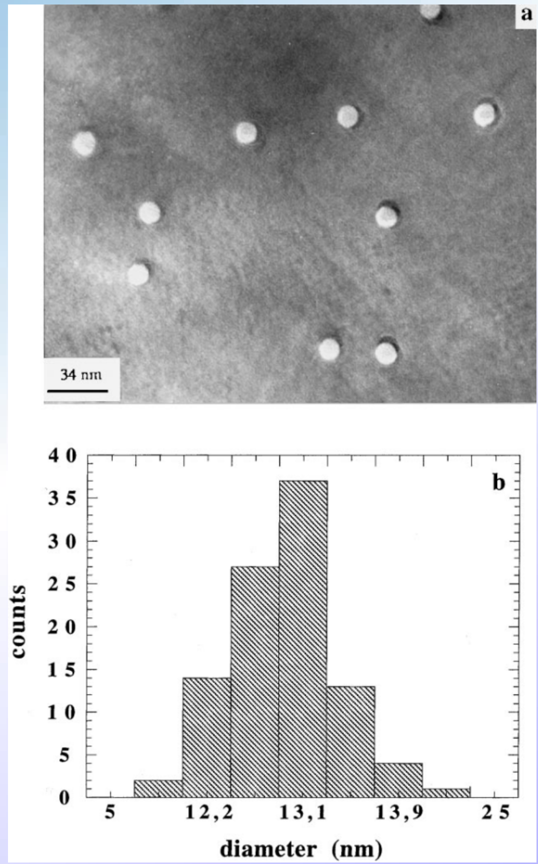

(a) Plane view micrograph of sapphire irradiated with 10^{10} $^{60}C^{2+}$ cm^{-2} at 30 MeV. (b) The histogram shows the repartition of the track diameters

S.M.M. Ramos et al. / NIM B 143 (1998) 319-332

Examination of the dense ionization effect in ceramics and oxides with heavy ions of fission fragments energy

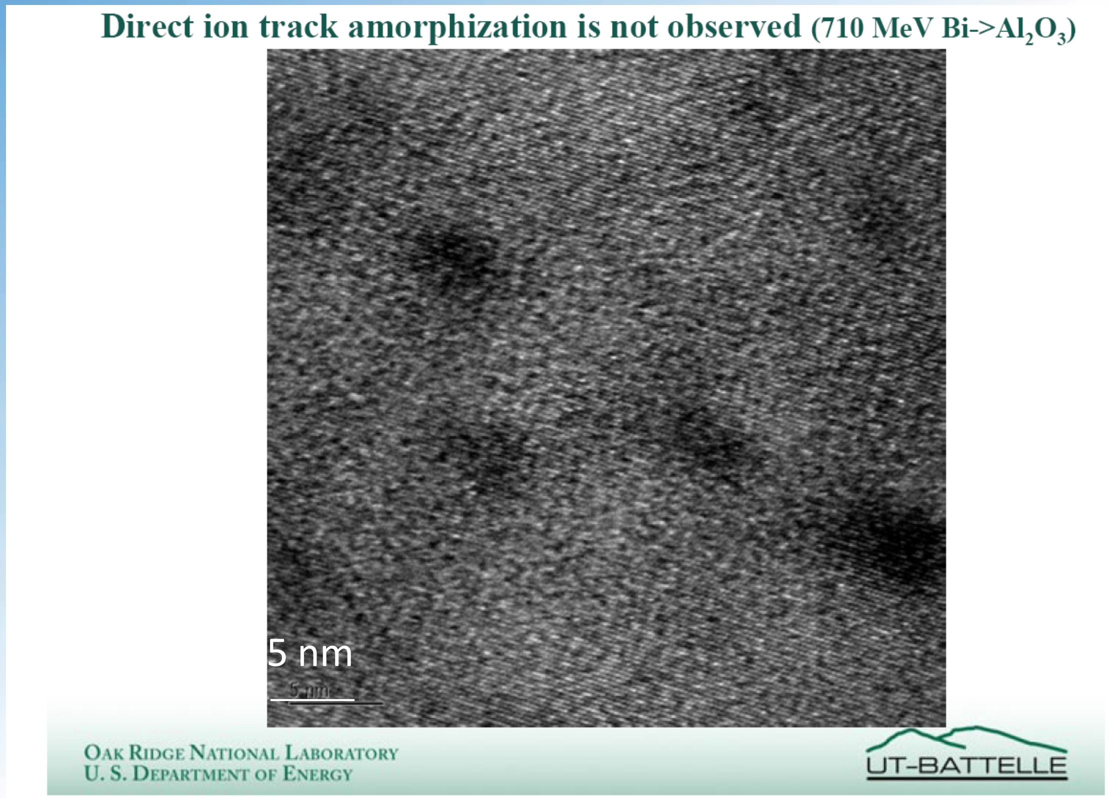

High-resolution lattice image of α-A_2O_3 irradiated with 710 MeV Bi ions (plan-view specimen). Ion fluence $7x10^{12}$ cm^{-2}. S_e =41 keV/nm

S. Zinkle, ORNL

Examination of the dense ionization effect in ceramics and oxides with heavy ions of fission fragments energy

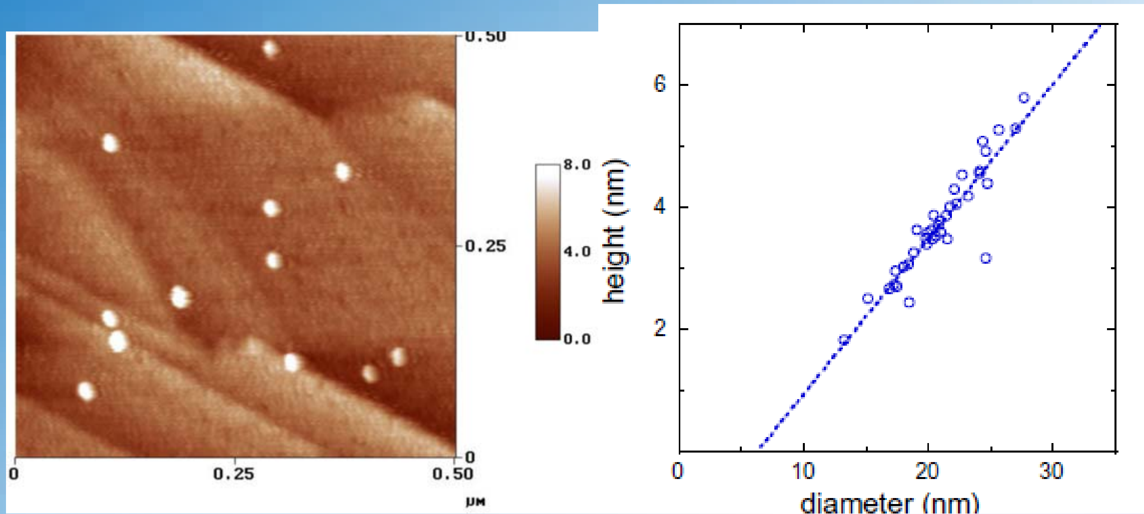

Surface topography image of Al_2O_3 irradiated by 1 MeV/u Au ions (5×10^9 ions/cm^2). Right: height versus diameter of hillocks.

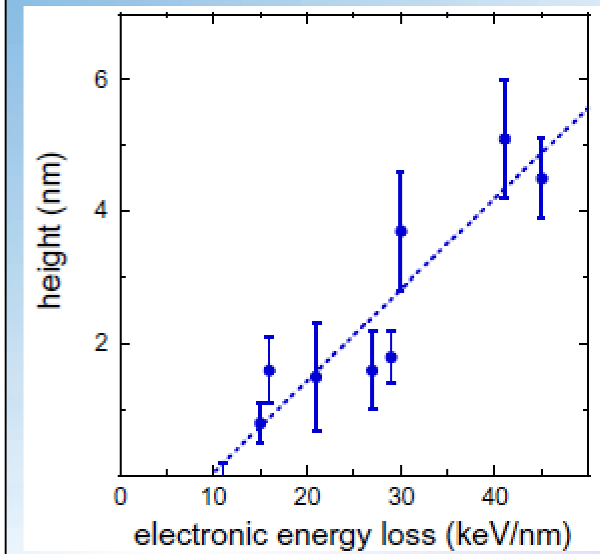

Mean hillock height versus electronic energy loss

Mean electronic energy loss threshold value for damage creation in Al_2O_3 is **9.5 ± 1.5 keV/nm**

N. Khalfaoui et al. NIMB, in press

Examination of the dense ionization effect in ceramics and oxides with heavy ions of fission fragments energy

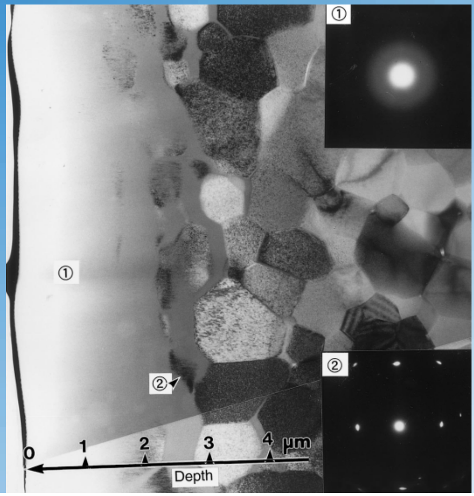

XTEM micrograph of Al_2O_3 irradiated with 85 MeV I^{7+} ions to 0.28×10^{15} cm^{-2}

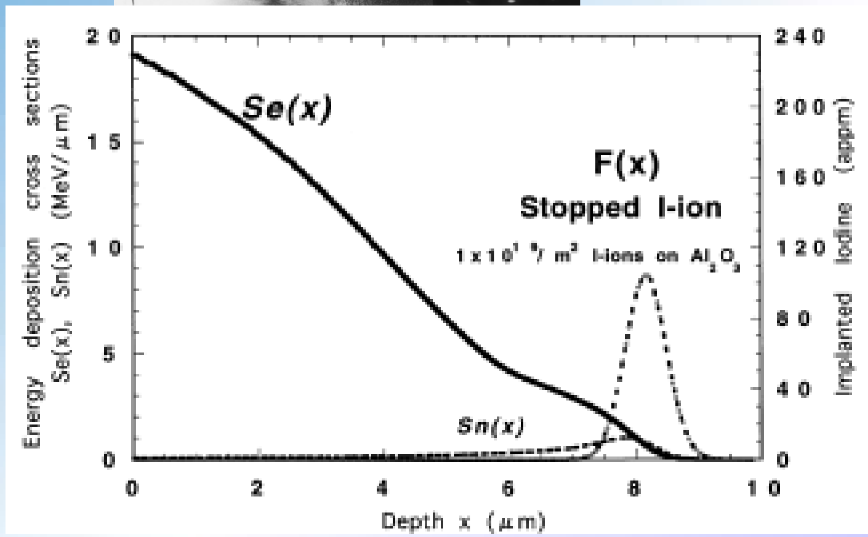

Nuclear and electronic stopping power depth profiles for 85 MeV I ions incident on Al_2O_3

T. Aruga et al. / NIM B(166-167)(2000),913-919

Examination of the dense ionization effect in ceramics and oxides with heavy ions of fission fragments energy

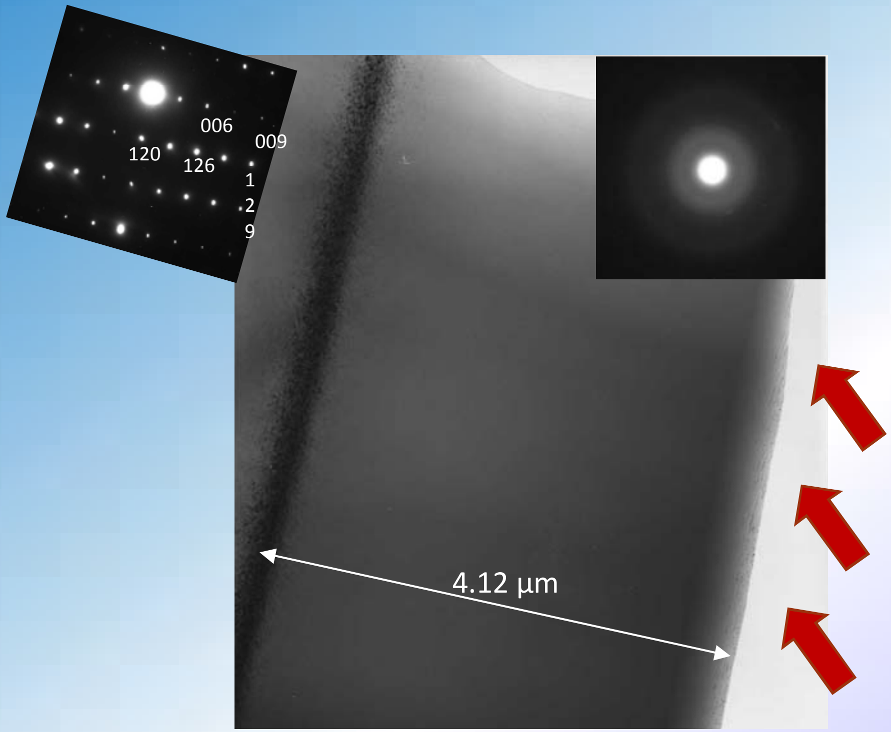

Ion irradiation in the track overlapping regime leads to amorphization of A_2O_3:Cr crystals

Xe ion beam

XTEM micrograph of A_2O_3:Cr single crystal irradiated with 167 MeV Xe ions.
$\Phi t = 2.9\times10^{13}$ cm^{-2}, T=80 K, ion beam incidence angle 30^o, $R_p \approx 5$ µm

V.A. Skuratov et al . NIMB. B 268 (2010) 3023

Examination of the dense ionization effect in ceramics and oxides with heavy ions of fission fragments energy

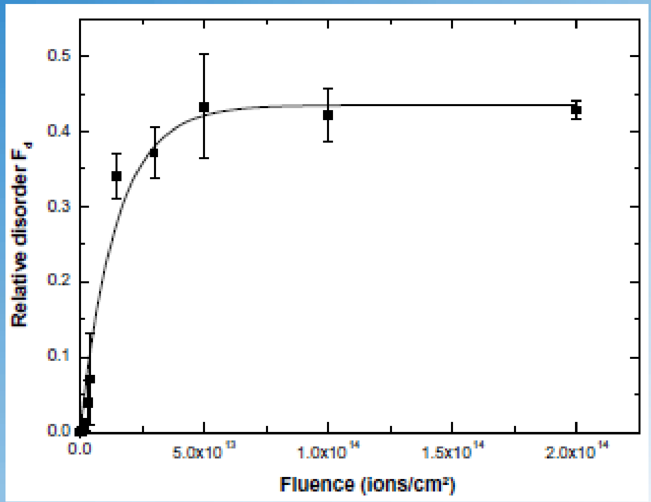

Fluence dependence of the relative disorder in irradiated sapphire

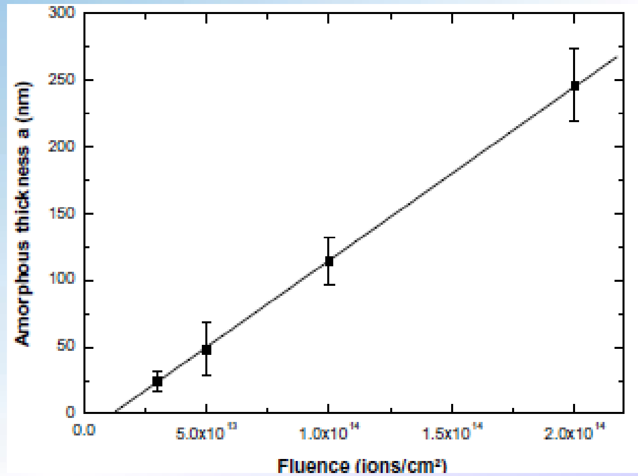

Evolution of the completely amorphous thickness a versus fluence deduced from RBS-C measurements.

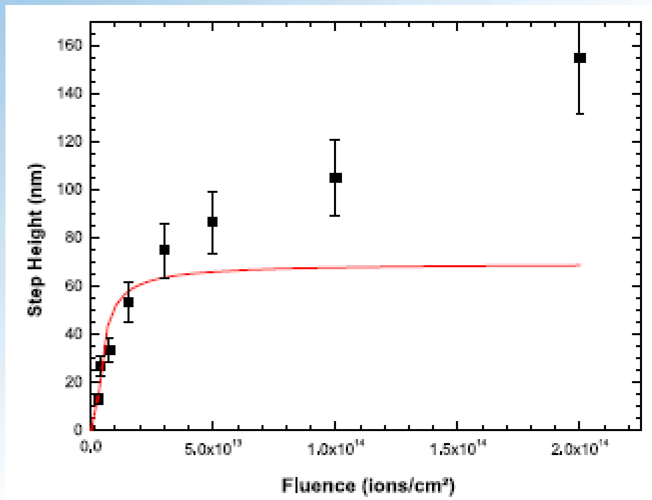

Step height of swelling versus ions fluence for α-Al_2O_3

$H=H_0(1-\exp(\sigma_{sw}\Phi)$

σ_{sw}- the effective swelling cross section

RBS-C analysis evidences the presence of two processes: partially disordered tracks first overlap, and in a second step an amorphous layer is growing linearly with fluence from the sample surface.

A. Kabir et al. / NIM B266(2008)2976–2980

Examination of the dense ionization effect in ceramics and oxides with heavy ions of fission fragments energy

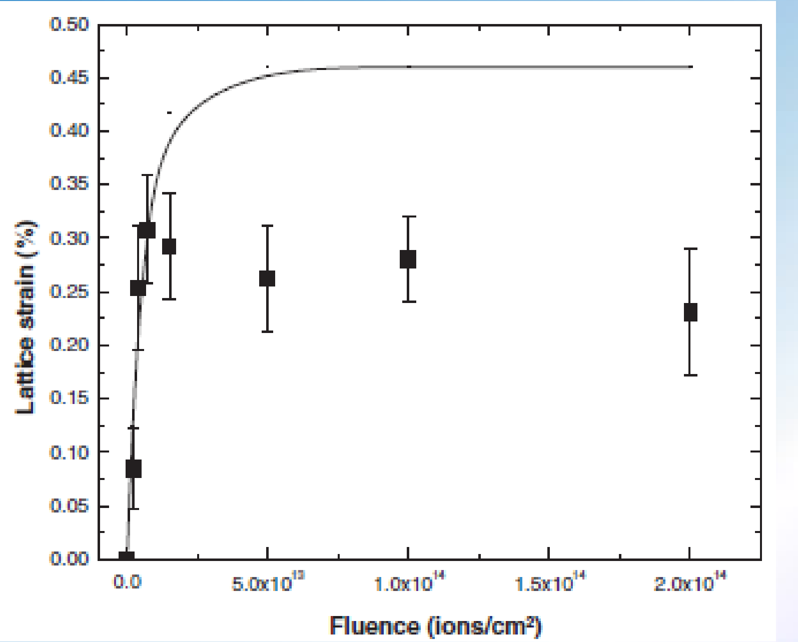

Variation of the lattice strain versus the fluence for α-Al_2O_3 irradiated with 90.3 MeV xenon ions

Swelling leads to build-up of mechanical stresses in the irradiating material

A. Kabir et al. / NIMB 268 (2010) 3195–3198

Examination of the dense ionization effect in ceramics and oxides with heavy ions of fission fragments energy

Swelling of insulators induced by swift heavy ions

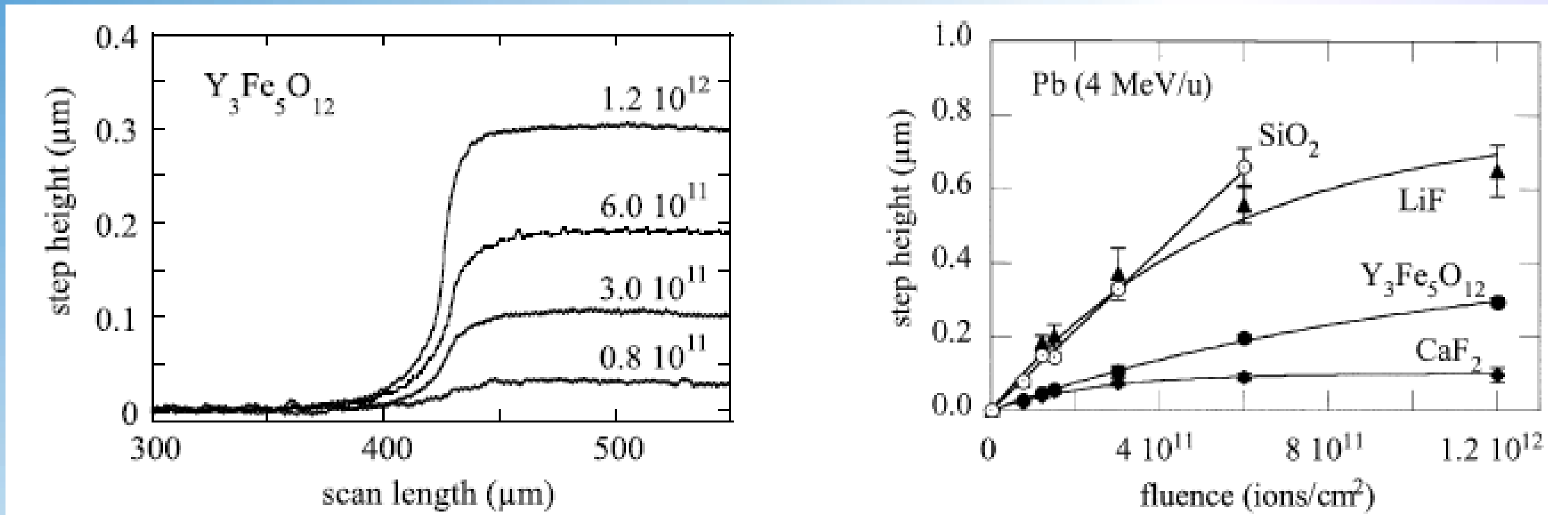

Profilometer scans for Pb (4 MeV/u) irradiations of $Y_3Fe_5O_{12}$ at different fluences (ions/cm^2).

Step height versus fluence for different crystals irradiated with Pb ions of 4 MeV/u

C. Trautmann et al. / NIMB 191 (2002) 144–148

Examination of the dense ionization effect in ceramics and oxides with heavy ions of fission fragments energy

yttrium stabilized zirconia (YSZ)

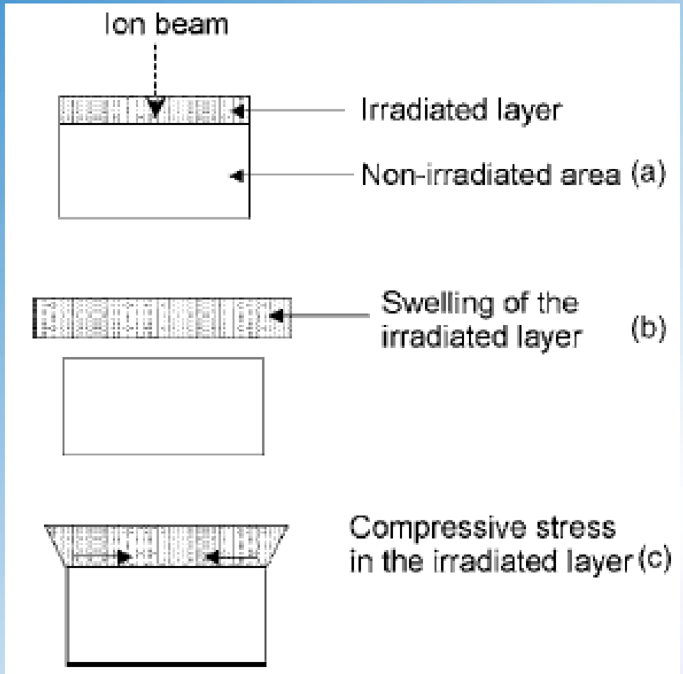

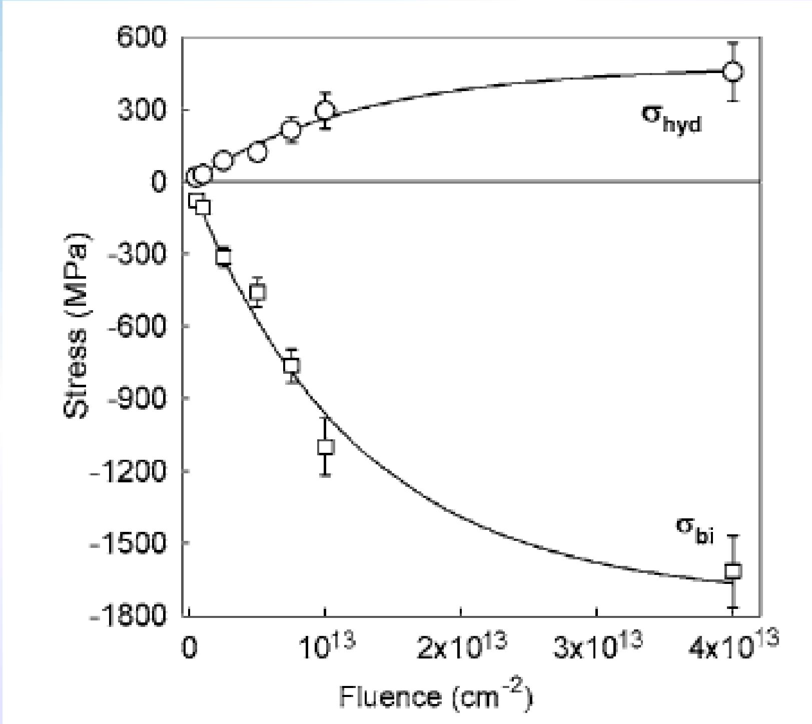

Variation of the hydrostatic and biaxial stress components in CSZ irradiated with 940 MeV Pb ions.

Sattonnay et al. J. Appl. Phys. ***101****, 103516 2007*

Examination of the dense ionization effect in ceramics and oxides with heavy ions of fission fragments energy

Crystalline to crystalline phase transformation induced in oxides by swift heavy ions

Yttrium oxide Y_2O_3 : cubic to the monoclinic phase (1-GeV Ta, 0.86-GeV Pb ions)

S.Hemon/ NIMB 146 (1998) 443-448

Pure zirconia ZrO_2 : monoclinic to the tetragonal phase (Se > 13 keV/nm)

A. Benyagoub / NIMB 206 (2003) 132–138

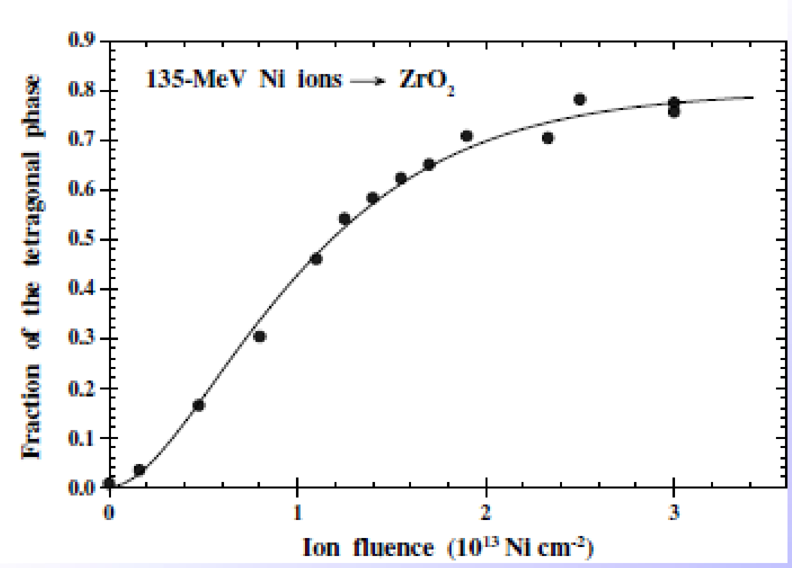

Evolution of the fraction of the tetragonal phase with the ion fluence in the case of the irradiation of pure zirconia with 135-MeV Ni ions.

Examination of the dense ionization effect in ceramics and oxides with heavy ions of fission fragments energy

yttrium stabilized zirconia (YSZ)

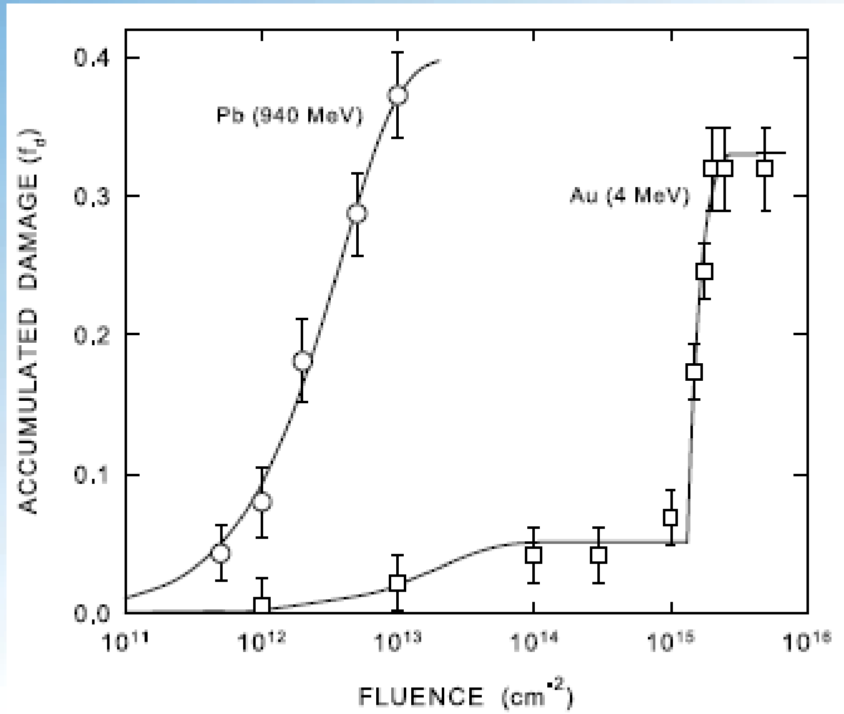

Accumulated damage (fd) versus ion fluence in YSZ crystals irradiated with 4MeV Au^{2+} and 940 MeV Pb^{53+} ions

S. Moll et al. / NIM B 266 (2008) 3048–3051

Examination of the dense ionization effect in ceramics and oxides with heavy ions of fission fragments energy

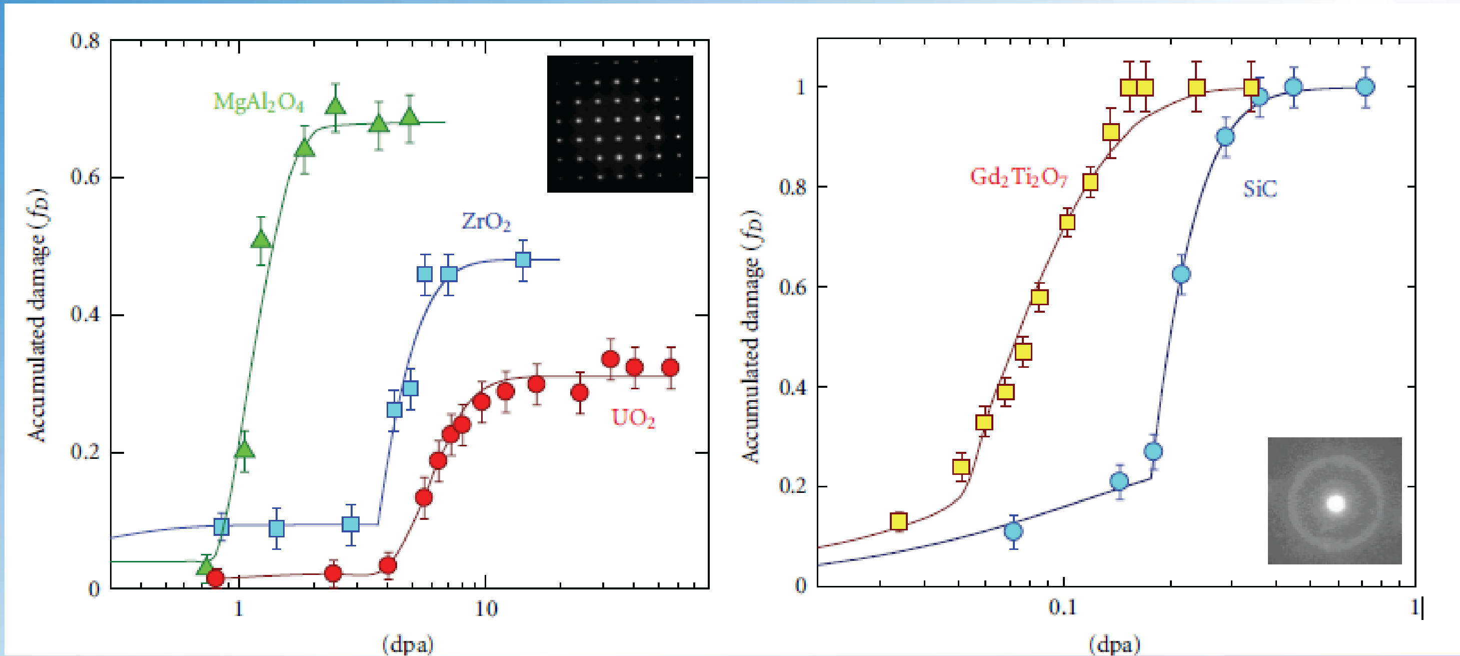

Accumulated damage (*fD*) versus ion fluence for nonamorphizable (a) and amorphizable (b) ceramics irradiated at RT with slow ions. Insets show TEM diffraction patterns recorded at the final fluences on both types of materials.

L. Thome et al. Advances in Materials Science and Engineering Volume 2012 (2012), Article ID 905474, 13 p.

Examination of the dense ionization effect in ceramics and oxides with heavy ions of fission fragments energy

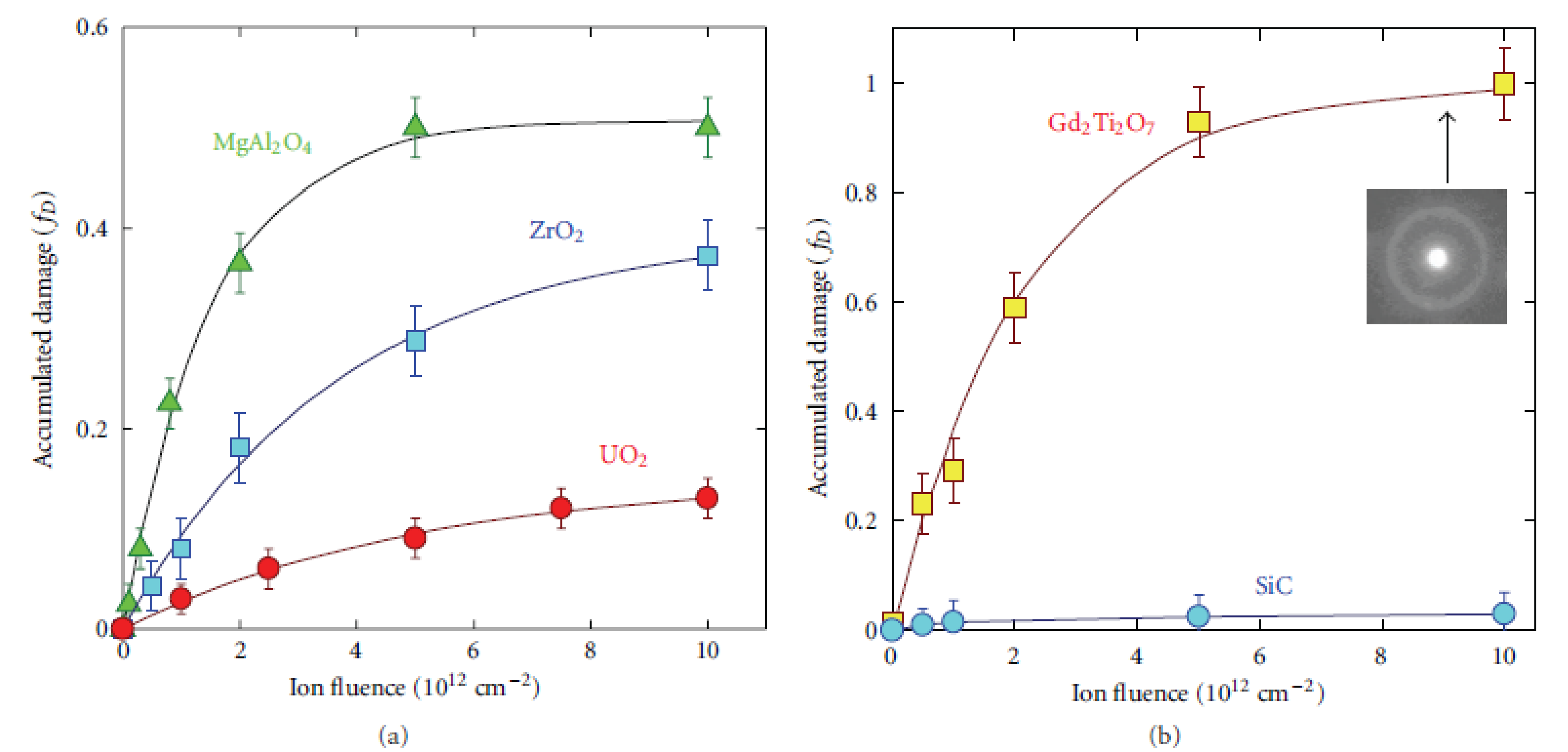

Accumulated damage (*fD*) versus ion fluence for nonamorphizable (a) and amorphizable (b) ceramics irradiated at RT with swift ions. The inset shows a TEM diffraction pattern recorded at the final fluence on $Gd_2Ti_2O_7$.

L. Thome et al. Advances in Materials Science and Engineering Volume 2012 (2012), Article ID 905474, 13 p.

Examination of the dense ionization effect in ceramics and oxides with heavy ions of fission fragments energy

Electronic sputtering of nitrides by high-energy ions

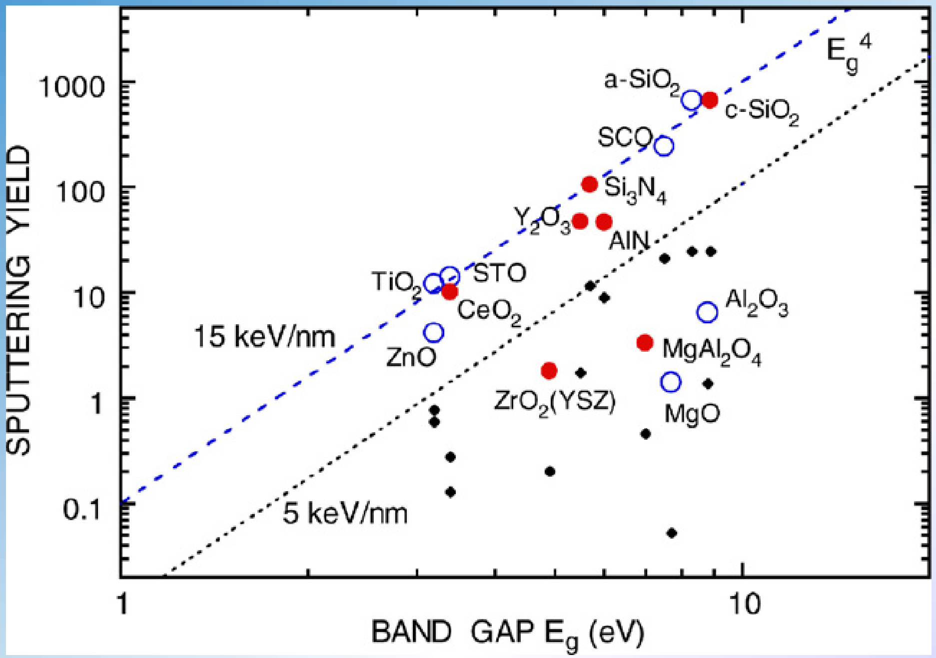

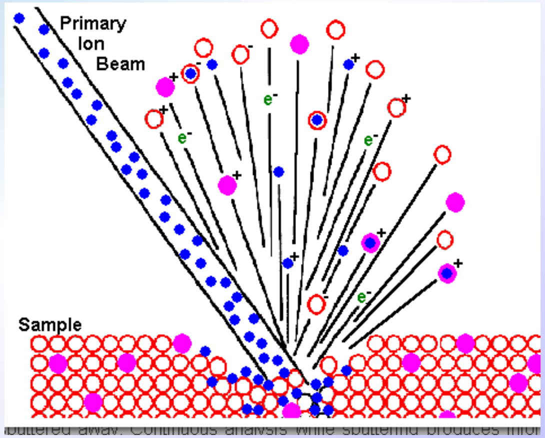

The sputtering yields are larger by 30 -2×10^3 than those of calculations based on the elastic collision cascades

Sputtering yields at Se = 15 (o) and 5 keV/nm (•) as a function of the band-gap
The electronic sputtering yields scale with the electronic stopping power as $\mathbf{S_e^n}$ with **n = 1.4–4**

N. Matsunami et al. / NIMB 209 (2003) 288-293
N. Matsunami et al. / NIMB 256 (2007) 333–336

Examination of the dense ionization effect in ceramics and oxides with heavy ions of fission fragments energy

Ionizing energy loss threshold values for latent track formation in nitrides and carbides

Material	S_{et}, keV/nm	Ref.
AlN	> 34	S.J. Zinkle, J.W. Jones, V.A. Skuratov. MRS Symposium Proceedings, Vol. 650, MR, Warrendale, PA, 2001, p. R3.19.1. S.J.Zinkle, V.A.Skuratov and D.T.Hoelzer. NIMB 191(2002) 758
	> 21.6	S. Mansouri et al. // NIMB 266(2008) 2814
BN	> 17.6	S. Mansouri et al. // NIMB 266(2008) 2814
SiC	>34	S.J. Zinkle, J.W. Jones, V.A. Skuratov. MRS Symposium Proceedings, Vol. 650, MR, Warrendale, PA, 2001, p. R3.19.1.
SiC Nano-SiC	> 22 > 17	A. Audren et al. // NIMB 267(2009) 976, NIMB 266 (2008) 2806
Nano-ZrN	> 49	A. Janse van Vuuren, V. A. Skuratov, V.V. Uglov (in press)
Si_3N_4	15	S.J. Zinkle, J.W. Jones, V.A. Skuratov. MRS Symposium Proceedings, Vol. 650, MR, Warrendale, PA, 2001, p. R3.19.1. S.J.Zinkle, V.A.Skuratov and D.T.Hoelzer. NIMB 191(2002) 758

Examination of the dense ionization effect in ceramics and oxides with heavy ions of fission fragments energy

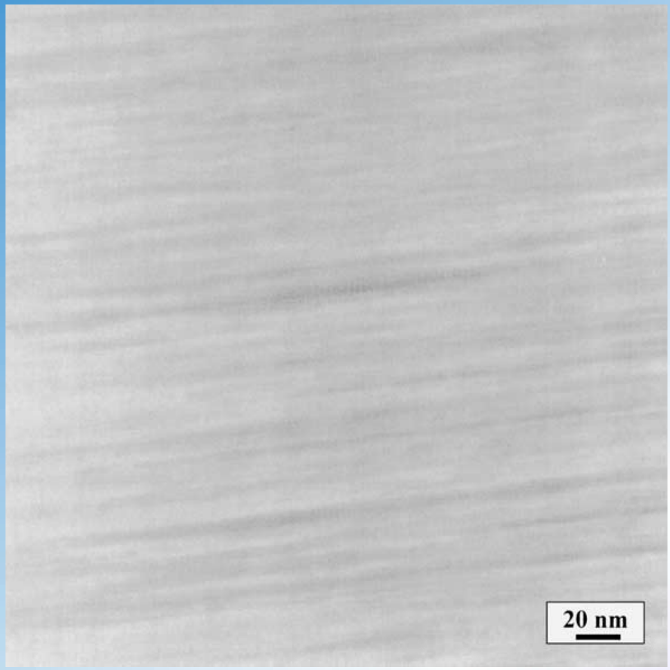

Mid-range microstructure of Si_3N_4 irradiated with 710 MeV Bi ions (cross-section specimen)

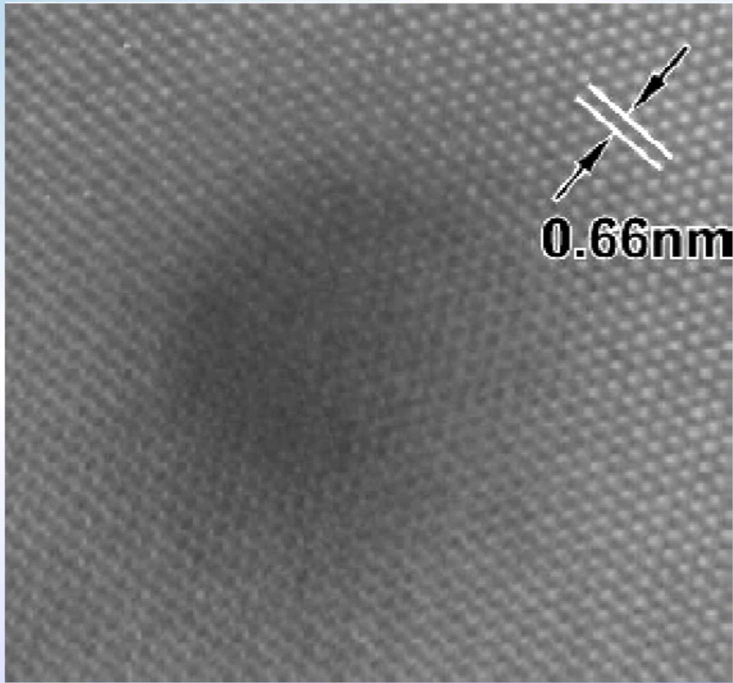

High-resolution lattice image of Si_3N_4 irradiated with 710 MeV Bi ions (plan-view specimen)

$S_{et} \approx$ **15 keV/nm**

S.J.Zinkle, V.A.Skuratov and D.T.Hoelzer. NIMB 191(2002) 758

Examination of the dense ionization effect in ceramics and oxides with heavy ions of fission fragments energy

Silicon carbide

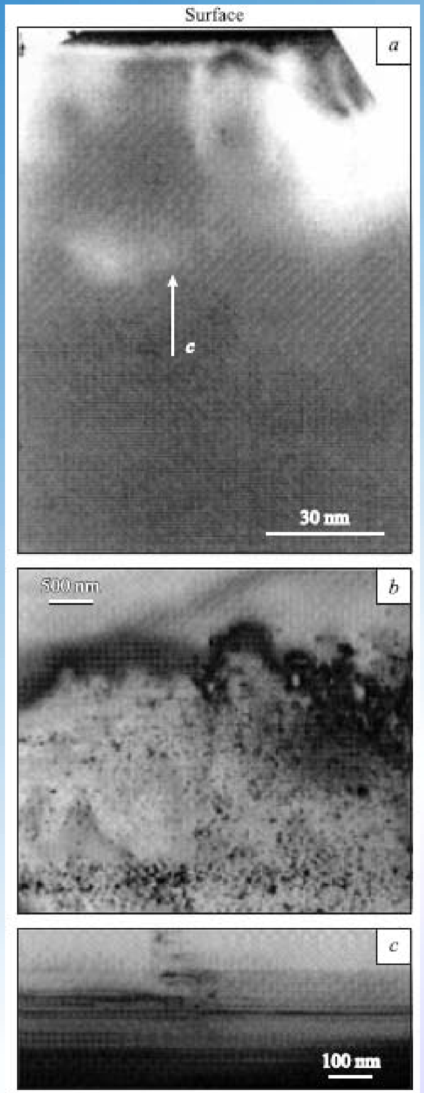

subsurface layer

end of range area as irradiated

end of range area annealing at 500C

XTEM images of *n*-4*H*-SiC CVD epitaxial layer irradiated with Bi ions. E = 710 MeV, 5 10^{10} cm^{-2}

CVD layer thickness – 26 μm
R_p = 29 μm

E.V. Kalinina, V.A. Skuratov et al. Semiconductors, v.41 (2007), iss. 4, 396

Examination of the dense ionization effect in ceramics and oxides with heavy ions of fission fragments energy

Dense ionization effect on pre-existing defect structure in SiC

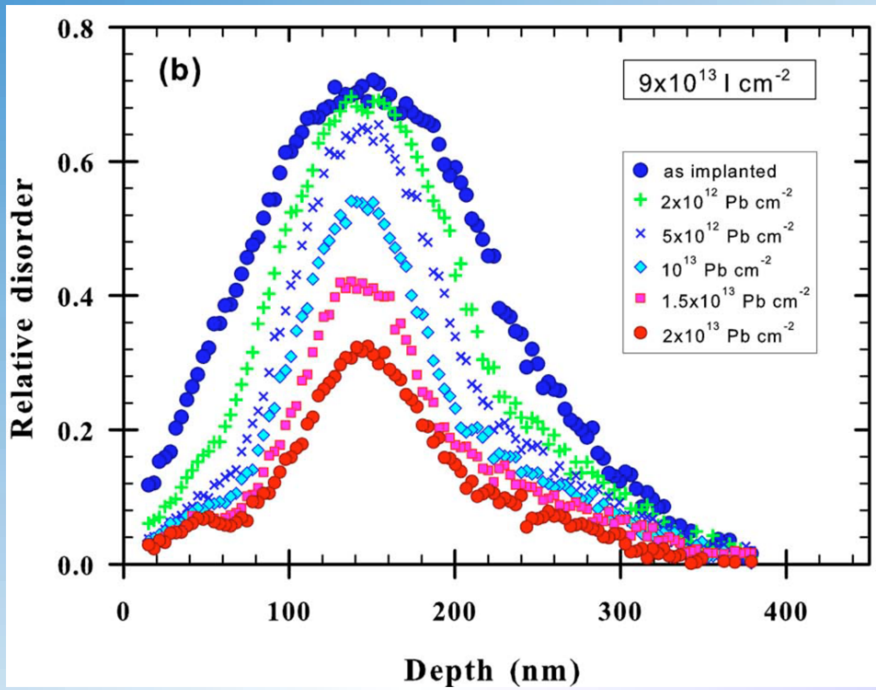

Epitaxial recrystallization induced by the irradiation with 827 MeV Pb ions of SiC samples previously damaged with 700 keV I at the fluence of 9×10^{13} I cm^{-2}

ion-beam-induced epitaxial crystallization (IBIEC effect)

A. Benyagoub and A. Audren J. Appl. Phys. ***106****, 083516 2009*

Thank you for your attention!